

# Revised Catalog of GALEX Ultraviolet Sources. I. The All-sky Survey: GUVcat\_AIS

Luciana Bianchi<sup>1</sup>, Bernie Shiao<sup>2</sup> and David Thilker<sup>1</sup>

bianchi@jhu.edu

## ABSTRACT

The Galaxy Evolution Explorer (GALEX) imaged the sky in two Ultraviolet (UV) bands, far-UV (FUV,  $\lambda_{eff} \sim 1528\text{\AA}$ ) and near-UV (NUV,  $\lambda_{eff} \sim 2310\text{\AA}$ ), delivering the first comprehensive sky surveys at these wavelengths. The GALEX database contains FUV and NUV images,  $\sim 500$  million source measurements and over 100,000 low-resolution UV spectra. The UV surveys are a unique resource for statistical studies of hot stellar objects,  $z \lesssim 2$  QSOs, star-forming galaxies, nebulae and the interstellar medium, and provide a road-map for planning future UV instrumentation and follow-up observing programs. We present science-enhanced, “clean” catalogs of GALEX UV sources, with useful tags to facilitate scientific investigations. The catalogs are an improved and expanded version of our previous catalogs of UV sources (Bianchi et al. 2011, 2014: BCScat). With respect to BCScat, we have patched 640 fields for which the pipeline had improperly coadded non-overlapping observations, we provide a version with a larger sky coverage (about 10%) by relaxing the restriction to the central area of the GALEX field to  $1.1^\circ$  diameter (GUVcat\_AIS\_fov055), as well as the cleaner, more restrictive version using only the  $1^\circ$  central portion of each field as in BCScat (GUVcat\_AIS\_fov050). We added new tags to facilitate selection and cleaning of statistical samples for science applications: we flag sources within the footprint of extended objects (nearby galaxies, stellar clusters) so that these regions can be excluded for estimating source density. As in our previous catalogs, in *GUVcat* duplicate measurements of the same source are removed, so that each astrophysical object has only one entry. Such unique-source catalog is

---

<sup>1</sup>Dept. of Physics & Astronomy, The Johns Hopkins University, 3400 N. Charles St., Baltimore, MD 21218, USA; <http://dolomiti.pha.jhu.edu>

<sup>2</sup>Space Telescope Science Institute, 3400 San Martin Dr., Baltimore, MD 21210

needed to study density and distributions of sources, and to match UV sources with catalogs at other wavelengths. The catalog includes all observations from the All-Sky Imaging Survey (AIS), the survey with the largest area coverage, with both FUV and NUV detectors exposed: over 28,700 fields, made up of a total of 57,000 observations (“visits”). The total area covered, when overlaps are removed and gaps accounted for, is 24,790 (GUVcat\_AIS\_fov055) and 22,125 (GUVcat\_AIS\_fov050) square degrees. The total number of “unique” AIS sources (eliminating duplicate measurements) is 82,992,086 (*GUVcat\_AIS\_fov055*) and 69,772,677 (*GUVcat\_AIS\_fov050*). The typical depth of the GUVcat\_AIS catalog is FUV=19.9, NUV=20.8 ABmag.

*Subject headings:* Astronomical Databases: surveys, catalogs; Stars: post-AGB, early-type; Galaxy: stellar content; Ultraviolet

## 1. Introduction.

Current observational astrophysics benefits from data mining of modern sky surveys, enabled by large-format detectors, improved instrument stability, and computational database facilities capable of easily handling large data volumes. At optical wavelengths, the relevance and variety of science outcomes from the first modern surveys of the sky, such as the Sloan Digital Sky Survey (SDSS), prompted new, more powerful surveys to be planned and built (e.g., Pan-STARRS, ESO-VISTA, SkyMAPPER, LSST...). At infrared, X-ray and  $\gamma$ -ray wavelengths, series of surveys with increasing quality, depth, and resolution have progressively advanced our view of several classes of sources most prominent in each range. At UV wavelengths, instead, only the Galaxy Evolution Explorer (GALEX) performed comprehensive sky surveys, with different coverage and depth (Morrissey et al. 2007; Bianchi 2009; Bianchi et al. 2011a; Bianchi 2014; Bianchi et al. 2014a). GALEX surveys therefore remain the most extensive resource in the UV for planning follow-up observations and missions, and for extracting science from the still largely unexplored database (for earlier, pioneering UV missions see e.g., Bianchi (2016)).

This work presents the latest version of the GALEX catalog of UV sources, **GUVcat**, that will facilitate statistical investigations involving UV measurements, and cross-matching with other samples. It follows, expands and improves the earlier versions by Bianchi et al. (2011a,b) and Bianchi et al. (2014a)(BCScat). We present here the catalog from the survey with the largest sky coverage; similar source catalogs from the deeper surveys, more limited in area coverage, will follow, as well as catalogs of UV variables, and a UV spectroscopic database.

The paper is arranged as follows: first we recall the characteristics of the GALEX instrument (Section 2), of the major surveys performed (Section 3), and of the GALEX data and photometry (Section 4) of relevance for catalog users. In Section 5 we describe the criteria used for construction of the new catalog and improvements with respect to previous versions, in Section 6 we give a statistical overview the catalogs’ source content, and provide relevant information for using the catalog, in Section 7 we explain the calculation of area coverage, and in Section 8 we discuss the distribution of sources across the sky as well as summarize useful caveats and suggestions for using this catalog and GALEX data. A detailed description of the procedure used to identify and remove duplicate measurements of sources is given in Appendix A. A complete list of the tags of catalog sources is given in Table 8 of Appendix B. Appendix C illustrates in more detail some caveats and the most relevant artifacts.

## 2. GALEX instrument and data characteristics

GALEX (Martin et al. 2005), a NASA *Small Explorer* class mission with contributions from the Centre National d’Etudes Spatiales of France and the Korean Ministry of Science and Technology, performed the first sky-wide Ultraviolet surveys. It was launched on April 28, 2003 and decommissioned by NASA on June 28, 2013. GALEX’s instrument consisted of a Ritchey-Chrétien–type telescope with a 50 cm primary mirror and focal length of 299.8cm. Through a dichroic beam splitter, light was fed to two detectors simultaneously, yielding observations in two broad bands: far-UV (FUV,  $\lambda_{eff} \sim 1528\text{\AA}$ , 1344-1786 $\text{\AA}$ ) and near-UV (NUV,  $\lambda_{eff} \sim 2310\text{\AA}$ , 1771-2831 $\text{\AA}$ ). GALEX had two observing modes, direct imaging and grism field spectroscopy. The FUV detector stopped working in May 2009; subsequent GALEX observations have only NUV data (Figure 1).

The GALEX field of view is  $\approx 1.2^\circ$  diameter (1.28/1.24 $^\circ$ , FUV/NUV), the spatial resolution is  $\approx 4.2/5.3''$  (Morrissey et al. 2007). For each observation, an FUV and an NUV image, sampled with virtual pixels of 1.5'' , are reconstructed from the photon list recorded by the two photon-counting micro-channel plate detectors. From the reconstructed image, the GALEX pipeline then derives a sky background image, by interpolating a surface from flux measurements in areas with no detected sources, and performs source photometry in various ways: aperture, psf, Kron-like elliptical (see Appendix B). Sources detected in the FUV and NUV images of the same observation are matched by the pipeline to produce a merged-source list (both bands combined) for each observation. We will return to this matching later.

To reduce local response variations, in order to maximize photometric accuracy, each

observation was carried out in “AIS mode” for most AIS data and with a  $1'$  spiral dithering pattern for MIS and DIS.<sup>1</sup> The surveys were accumulated by covering contiguous “*tiles*” in the sky, with series of such observations, sometimes repeated, called “*visits*”.

The Galactic plane was largely inaccessible during the prime mission phase because of the many bright stars that violated high-countrate safety limits. Such constraints were relaxed at the end of the mission. A survey of the Magellanic Clouds (MC), also previously unfeasible due to brightness limits, was completed at the end of the mission, when the initial count-rate safety threshold (Bianchi (2014); Simons et al. (2014); Thilker et al. (2017)) was lowered. Because of the FUV detector’s failure in 2009, these extensions include only NUV measurements (Figure 1).

### 3. The sky surveys

GALEX has performed sky surveys with different depth and coverage (Morrissey et al. (2007), Bianchi (2009)). The two detectors, FUV and NUV, observed simultaneously as long as the FUV detector was operational; however, there are occasional observations in which one of the two detectors was off (mostly FUV) due to brief shut-down episodes, even in the early part of the mission; in addition, in some observations the FUV and NUV exposure times differ (see Bianchi et al. 2014a, in particular their Table 1 and Fig. 2).

The surveys with the largest area coverage are the All-Sky Imaging survey (AIS) and the Medium-depth Imaging Survey (MIS): the sky coverage is shown in Figure 1. Exposure times slightly vary within each survey, around the respective nominal exposures of 100 sec for AIS, which corresponds to a detection limit ( $5\sigma$ ) of FUV $\sim$ 20/NUV $\sim$ 21 ABmag, and 1500 sec for MIS, corresponding to a depth of  $\sim$ 22.7 ABmag in both FUV and NUV. The Deep Imaging Survey (DIS) accumulated exposures of the order of several tens of thousand of seconds in selected fields (for example, for a 30,000 sec exposure, the depth reached is  $\sim$ 24.8/24.4 ABmag in FUV/NUV). In addition, the “Nearby Galaxies Survey” (Bianchi et al. 2003, Gil de Paz et al. 2007), dedicated to mapping large nearby galaxies, covered initially 436 fields at MIS depth, but hundreds of additional nearby galaxies were mapped by GALEX, as part of MIS or other surveys (see also Section 6.1). Other observations were obtained during guest investigator (GI) programs, and for other targeted regions such as,

---

<sup>1</sup>A trailing mode, rather than the spiral dithering pattern, was instead used for the latest, privately-funded observations, to cover some bright areas near the MW plane. These latest data currently are not in the public archive. Also, a so-called Petal-mode was used in special cases. The spiral dithering pattern was used for most of the science data, and for all of the data used in this catalog.

for example, the Kepler field (e.g., Smith et al. (2014)).

The current GALEX database (data release GR6plus7) contains 582,968,330 source measurements resulting from a total of 100,865 imaging *visits*; most of these source measurements are from observations with both FUV and NUV detectors on (64551 *visits*, 47239 of which from the AIS survey). Figure 1 shows the sky coverage of all GALEX observations performed with both FUV and NUV detectors on (right panel), and in NUV regardless of FUV-detector status (left panel). The figure does not include the last NUV trailed observations (the privately-funded “CAUSE” observing phase, conducted in scan mode).

#### 4. GALEX data and photometry

GALEX data include images through either direct imaging or grism, and associated photometry from the pipeline or extracted spectra respectively. High-level science products (HLSP) have also been released (Bianchi et al. 2011a), and unique source catalogs (i.e., with no duplicate observations of the same source, Bianchi et al. (2011a, 2014a): BCScat), these are available at MAST and Vizier, and are precursors of the present catalog.

The photometry calibration for any data release uses the zero points of Morrissey et al. (2007), any subsequent pipeline updates were reflected in revised extracted source count-rates (CTR), so that the zero points remained unchanged. On the AB magnitude scale, the GALEX magnitudes are defined as:

$$\text{UV\_mag} = -2.5 \times \log(\text{CTR}) + \text{ZP} \quad (\text{AB mag}) \quad (\text{eq. 1})$$

where CTR is the dead-time corrected, flat-fielded count rate (counts s<sup>-1</sup>) and the zero-point values are ZP<sub>FUV</sub>=18.82 and ZP<sub>NUV</sub>=20.08.

The transformations to Vega magnitudes are (Bianchi 2011) :

$$\text{FUV\_mag}_{\text{Vega}} = \text{FUV\_mag}_{\text{AB}} - 2.223 \quad (\text{eq. 2})$$

$$\text{NUV\_mag}_{\text{Vega}} = \text{NUV\_mag}_{\text{AB}} - 1.699 \quad (\text{eq. 3})$$

In Sections 4.1 to 6.1 we discuss additional details and relevant caveats for using GALEX data. Practical advice on use of GALEX data and this catalog is summarized in Section 8.2.

#### 4.1. Bright sources

High count-rates from UV-bright sources cause non-linearity in the response, or saturation, due to the detector’s dead-time correction being overtaken by the photon arrival rate. Morrissey et al. (2007) reported non-linearity at a 10% rolloff to set in at 109 counts  $\text{s}^{-1}$  for FUV and 311 counts  $\text{s}^{-1}$  for NUV. These countrates correspond to FUV\_mag=13.73 ABmag ( $\sim 1.53 \cdot 10^{-13} \text{ erg s}^{-1} \text{ cm}^{-2} \text{ \AA}^{-1}$ ) and NUV\_mag=13.85 ABmag ( $\sim 6.41 \cdot 10^{-14} \text{ erg s}^{-1} \text{ cm}^{-2} \text{ \AA}^{-1}$ ). A correction for non-linearity is applicable over a limited range, beyond which the measured countrate saturates and the true source flux is no longer recoverable (see their Figure 8). The bright-object limit during the primary mission was 30,000 counts  $\text{s}^{-1}$  per source, corresponding to  $\sim 9^{\text{th}}$  ABmag for NUV ( $\sim 7 \cdot 10^{-12} \text{ erg s}^{-1} \text{ cm}^{-2} \text{ \AA}^{-1}$ ) and 5,000 counts  $\text{s}^{-1}$  per source in FUV (ABmag  $\sim 9.6$ ,  $\sim 6 \cdot 10^{-12} \text{ erg s}^{-1} \text{ cm}^{-2} \text{ \AA}^{-1}$ ). Such limits were relaxed at the end of the mission.

In addition to the non-linearity for sources with high CTR, the total CTR over the entire field affects the stim-pulse correction, which in turn affects the correction for non linearity. We refer to Thilker et al. (2017) for details of the issue, and recipe for correction.

The calibration of GALEX fluxes is tied to the UV standards used for HST (Bohlin 2001). However, all but one of the white dwarf (WD) standard stars have GALEX count-rates in the non-linear regime. Camarota & Holberg (2014) derived an empirical correction to the GALEX magnitudes in the non-linear range, using a well studied sample of WDs with previous UV spectra and model atmospheres. Their correction is valid in the bright-flux regime as specified in their work, but would diverge if extrapolated to fainter fluxes. Further refinements of the calibration have not yet been explored to our knowledge. In future works we will examine the stability of the response at very high countrates (Bianchi et al. 2017a; de la Vega & Bianchi 2017).

#### 4.2. Crowded fields

Source detection and photometry measurements performed by the GALEX pipeline become unreliable where sources are too crowded relative to the instrument’s resolution. Conspicuous examples include stellar clusters in the Milky Way (Figure 2), fields in or near the Magellanic Clouds (Simons et al. 2014; Bianchi 2014), and nearby extended galaxies (Section 6.1). The pipeline, designed for the general purpose of detecting both point-like and extended sources (such as galaxies, typically with an elliptical shape), sometimes interprets two or more nearby point sources as one extended source; this seems to occur in crowded regions, as Figure 2 shows. Note that, in some crowded fields, at times the pipeline fails to

resolve even point-like sources with separation comparable to, or larger than the instrumental resolution; see Figure 2 for an example, or Figure 3 of Simons et al. (2014) for a Magellanic Cloud field. In extended galaxies, the local background of diffuse stellar populations may compound the crowding around clustered sources or bright star-forming complexes.

In extended galaxies, because UV fluxes are sensitive to the youngest, hottest stars, which are typically arranged in compact groups within star-forming regions, UV-emission peaks are identified by the pipeline as individual sources and some star-forming structures may be shredded in individual peaks, or tightly clustered sources may be merged into an extended source. In other cases, the extended emission of the central galaxy disk is often interpreted as a single extended source. In many cases, the result from the pipeline is a single measurement of a large central area and an overdensity of sources in the outer disk. An example is shown in Fig.5. Custom measurements are needed in extended galaxies, with special care to background subtraction (e.g., Kang et al. (2009); Efremova et al. (2011); Bianchi et al. (2014b); Thilker et al. (2007, 2017)). Useful tags to identify such cases are described in Section 6.1.

For consistency, and completeness, all AIS measurements from the master database with both FUV and NUV exposures  $>0$  seconds were used to produce our GALEX source catalogs GUVcat\_AIS. Large galaxies, stellar clusters, and MC fields<sup>2</sup> were not excluded, to avoid introducing arbitrary gaps in the catalog coverage, because choice of which regions must be excluded depends on the specific science application and the characteristics of the sources to be analyzed (e.g., magnitude range, Bianchi et al. (2011b)). As with every large database, it is ultimately the user’s choice (and responsibility) to check crowded or problematic regions or extended objects, and exclude such regions if needed, or carefully check the photometry if these areas cannot be excluded (see Section 6.1), and use specific custom-vetted photometry catalogs for these particular areas when necessary. For the Magellanic Clouds (MC), initial custom photometry was performed by Simons et al. (2014); the final and complete version of the MC catalog is published by Thilker et al. (2017) and should be used in these regions, instead of GUVcat or the database products.

---

<sup>2</sup>We recall that only the periphery of the MC has both FUV and NUV exposures; the coverage of the inner portions has mostly NUV data (Bianchi 2014; Simons et al. 2014), and therefore was not included in our catalog; the whole MC catalog, from custom-vetted photometry, will be published elsewhere (Thilker et al. 2017)

## 5. The UV source catalog.

For several sources there are multiple measurements in the GALEX master database, due to repeated observations of the same field, or overlap between contiguous fields. For studies involving UV-source counts, or to match UV samples with catalogs at other wavelengths, one needs to eliminate repeats, as well as artifacts. Therefore, we have constructed catalogs of *unique* UV sources, eliminating duplicate measurements of the same object. Separate catalogs were constructed for AIS and MIS, because of the  $\sim 2$ -3 mag difference in depth. The catalog presented here is an expanded and improved version of “BCScat” published by Bianchi et al. (2014a), who also presented the first sky maps showing density of UV sources with various cuts. An earlier version, based on the fifth data release (GR5), was published by Bianchi et al. (2011a), who extensively discussed the criteria for constructing GALEX source catalogs and matched catalogs between GALEX and other surveys. Bianchi et al. (2011b) presented distributions of density of sources as a function of Galactic latitude, magnitude, and colors. We refer to these papers for useful presentations of the UV source distributions across the sky, and in magnitudes and colors; such considerations will not be repeated here because the overall statistics will appear very similar, but we strongly advise to use the catalog presented here for better quality and completeness. The improvements with respect to the earlier versions are described in the next section. Bianchi et al. (2011a) also released matched GALEXxSDSS catalogs, and Bianchi et al. (2011b) presented matched GALEXxGSC2 catalogs. Work on source classification from the matched catalogs was presented by Bianchi (2009) and Bianchi et al. (2011a, 2009, 2007, 2005). The earlier versions of the unique-source catalogs (Bianchi et al. 2011a, 2014a) are superseded by GUVcat presented here. Matched catalogs of GUVcat with SDSS, PanSTARRS, 2MASS, WISE, and Gaia will be released by Bianchi et al. (2017b).

In the GALEX database, an FUV magnitude with value of -999 means either that the FUV detector was on and the source was detected in NUV but too faint in FUV to be measured, or that the FUV detector was off. In order to examine and classify sources by color, and the relative fraction of sources with different colors, Bianchi et al. (2014a, 2011a) restricted the catalogs to those observations in which both detectors were exposed. We do the same here. In addition, our previous catalogs were conservatively restricted to measurements within the central  $1^\circ$  diameter of the field of view, to exclude the outer rim, where distortions prevent position and photometry of sources to be derived accurately, and counts from rim spikes cause numerous artifacts to intrude the source list. In the present version we again offer a catalog restricted to sources within  $0.5^\circ$  from the field center, GUVcat\_AIS\_050, and also a version relaxing this limit to  $0.55^\circ$ , GUVcat\_AIS\_055, to reduce gaps in area coverage, as described in Section 5.2 and 7. Sections 5 and 8.2 clarify which catalog is preferable depending on the science purpose. The present catalog includes all AIS fields with both

FUV and NUV exposed.<sup>3</sup>

### 5.1. Patching and updating BCScat

The initial need for patching *BCScat* came from the discovery that in some fields the GALEX pipeline had coadded observations from different *visits* which are largely *not* overlapping. GALEX observed each field (termed “*tile*” in the database) in one or more “*visit*” (composed of one or more “subvisit”); the partial-exposure images (*visits*) that passed the either automated or manual quality test (“QA”) were coadded, and “*coadd*” products (images, photometry) from the pipeline were entered in the database; the exposure time listed for the *coadd* is the sum of the partial exposures that were combined. A data-set is listed as “*coadd*” in the database even if it consists only of one *visit*. The *coadd* products are the default data level accessed by browsing the GALEX database with *GALEXview* (galex.stsci.edu/galexview). For constructing the catalog, and for most other purposes, using the *coadds* as a starting point is the best option since they provide the total exposure available for each field, with all *visits* already coadded. Our previous catalogs were therefore constructed combining sources from the *coadds*, and so is the catalog being released with this paper, with the exceptions described below.

The UV source catalog BCScat\_AIS (Bianchi et al. 2014a) was constructed from the 28,707 AIS *coadds* with both FUV and NUV *total* exposures  $>0$ . These *coadds* are made up of 57,000 *visits* (47,239 of which have both detectors exposed). We discovered however that in some GALEX AIS fields the pipeline had coadded *visits* centered at significantly differing positions, up to 26.8’ apart (which means, in this extreme case, almost no overlap). The pipeline then places the nominal center of the resulting *coadd* in between the centers of the merged *visits*, compounding the problem and making some critical tags useless (misleading). *Coadds* made of non-overlapping *visits* cause three potential problems, affecting any analysis, and all previous catalogs. To illustrate these problems we show an example, *tile* AIS\_480, in Fig. 3. In this case the database has merged two *visits*: one with both detectors exposed (shown as green dots in Fig. 3) and one with only the NUV-detector exposed (yellow dots). The database sources associated with this *tile*, i.e. the *coadd*, are shown in purple. The total exposure time given in the database is the sum of the exposures of

---

<sup>3</sup>BCScat\_AIS includes 28,707 AIS fields with both FUV and NUV exposed, covering a unique area of 22,080 square degrees as they were restricted to sources within the central  $1^\circ$  of each field, and BCScat\_MIS includes 3,008 MIS fields covering a total 2,251 square degrees. The previous catalogs of Bianchi et al. (2014a) (“BCScat” in MAST casjobs: <https://archive.stsci.edu/prepds/bcscat/> and Vizier) contain  $\approx 71$  million AIS and  $\approx 16.6$  million MIS sources.

the two *visits*, hence all the AIS\_480 sources (the purple dots) appear to have FUV exposure equal to that of the first *visit*, and NUV exposure equal to the sum of the two *visits*. But this is only true in the area of overlap of the two *visits*, which is very small in this case. In the yellow-dot-only area (portion of *visit* 2 not overlapping with *visit* 1), sources have FUV\_mag=-999 (i.e., non-detection), but they appear to have an FUV exposure  $>0$  (as the same exposure is given for the entire *coadd*), therefore they would be erroneously interpreted as having FUV flux below the detection threshold, while in fact they have no FUV data. In the green-dot-only area, sources appear to have an NUV exposure equal to the sum of the two *visits*, while they only have the exposure time of *visit* 1. Such improper *coadds* then introduce two biases when one selects - as we do in our previous, and current, catalogs - only fields with both detectors exposed, and we include for each field only sources within a certain radius from the field center to avoid rim artifacts and poor source photometry in the outer edge of the field of view (f.o.v.). First, the green-only sources, that would meet our catalog selection criteria (both detectors exposed), are not included in the catalog, because the center of the tile is the center of the *coadd* (in Figure 3-top black dots are the sources within  $0.5^\circ$  from the *coadd*'s field center). Second, some yellow-only sources (within the  $0.5^\circ$  circle from the *coadd* center) intrude the sample in spite they actually have no FUV exposure. The consequences will be for example that the ratio of FUV detections over NUV detections will be incorrect, and so any interpretation of UV color. In sum, these “bad *coadds*” cause: (i) loss of sources that should have been included, (ii) intrusion of sources not meeting the criteria, and (iii) misleading exposure times for the included sources. In addition, and worst of all, (iv) our criterion of limiting the catalog to sources within  $0.5^\circ$  from the field center, intended to exclude the numerous rim artifacts and distorted sources along the edge of the fields, is nullified by the *fov\_radius* value being assigned by the pipeline with respect to the centering of the *coadd*: Fig. 3 shows that the merged sources within  $0.5^\circ$  from the *coadd* center include part of the rim of both *visits*. In fact, by imposing a limit of  $fov\_radius \leq 0.5^\circ$ , we would expect no sources with rim artifact flag in the catalog; instead, there are 116,530 sources with *fuv\_artifact*=32 and 74,579 with *nuv\_artifact*=32 in BCScat\_AIS. These were introduced by the *coadds* in which non-overlapping *visits* had been merged by the pipeline (hereafter *bad coadds*). This problem had never been reported previously to our knowledge. When we discovered it, we undertook an effort to identify all the *bad coadds* in the database, and patch the catalogs. The result is the GUVcat\_AIS presented here.

The first step for constructing a revised catalog was therefore to identify the *bad coadds*, and to use the data from the corresponding individual *visits* instead of the *coadd* in such cases. To identify the *bad coadds*, we compared the center of each of the 28,707 AIS *tiles* with the centers of their associated *visits* (i.e., the *visits* used by the pipeline to build each *coadd*). For all cases where the center of one or more of the associated *visits* differs by

more than  $5'$  from the center of the coadded *tile*, we discarded the *coadd* and ingested in the catalog the corresponding *visits* (those that satisfy the criteria of both detectors being exposed). In this way we ensure that an FUV non-detection in the catalog is an actual non-detection and not a non-exposure, that the exposure times are correct, and that the centers correspond, within a given tolerance, to the actual centers of the observation (*visit*) so there is no loss of good sources, and no inclusion of rim artifacts (see also next section). We chose a tolerance of  $5'$  between *visit* centers, as a good compromise to use as many as possible of the *coadds* (which offer the most exposure available in each field) without introducing the negative effects described above.

Out of a total 28,707 AIS fields with both FUV and NUV exposure  $>0$ , made up of 57,000 *visits*, there are 640 *bad coadds*<sup>4</sup>, made up of 1195 *visits*. Of these *visits*, 886 have both FUV and NUV exposed: these have been used to construct the new catalog, in place of their corresponding 640 *bad coadds*. The *bad coadds* identified in this way are spread all across the sky, therefore it was not possible to simply patch a subset of the previous (BCScat) catalog by removing the *bad coadds* and replacing them with data from the individual *visits*, because to construct the unique-source catalog duplicate measurements of the same source had been identified and removed. Some of the *bad coadds* overlap with other (good) fields, and the procedure constructing the catalogs eliminates duplicate measurements from overlapping fields.

We therefore constructed a new catalog, GUVcat\_AIS, using all the “good” *coadds* (28067, with both FUV and NUV exposed, *visit* positions within each *coadd* differing by no more than  $5'$ ), and for the *bad coadds*, the individual *visits* of that *tile* instead. Table 4 (electronic only) lists the centers of the *tiles* used to construct the new catalog, and specifies whether *coadd* (“C”) or *visit* (“V”) photometry was used. The 640 *bad coadds* are listed in Table 5 (electronic only); we release this list too, because it may be of general interest, in providing to users of the GALEX database a quick quality check of the data they use. Because of its potential more general use, in Table 5 we include all AIS *coadds* and *visits* regardless of exposure, although in our catalog we only retain observations with both detectors exposed. These are easy to identify, having both exposure times  $>0$ , and are indicated as ‘G’ in the last column of the table (they were included in BCScat), ‘N’ indicates those not included.

In the next section we describe the criteria used to construct the new catalog, which largely follows our previous recipe (Bianchi et al. 2011a, 2014a), with several improvements.

---

<sup>4</sup>we term *bad coadd* a field in the database which was made combining *visits* of which at least one has its center  $>5'$  away from the *coadd*’s center

Five of the *coadds*, which appear to have both FUV and NUV exposure, were not replaced by their individual *visits* because each one consists only of two *visits*, non overlapping, one exposed only in NUV and one exposed only in FUV. These *coadds* were included in BC-Scat, but are excluded in the present catalog, and not replaced by *visits*; They have the following *photoextractid*: 6385728408348786688, 6385728422307430400, 6386256187888762880, 6386748750844395520, 6386748759434330112. These entries are marked with 'N' in the last column of Table 5. For one of these fields the difference between the center of the two visits is only 5.4' : this implies that most of their sources (except for an outer annulus) may have good measurements in both filters. We had nonetheless to apply a consistent criterion to discard *bad coadds*, therefore these data are not included in GUVcat\_AIS.

To summarize: in the GALEX database there are 28,707 AIS fields (*coadds*) that appear to have both FUV and NUV exposure  $> 0$ ; we examined the distance between the center of each *coadd* and the center of the *visits* which were combined to produce it, and found 28,067 *good coadds* (distance between all *visits* of the same *coadd*  $< 5'$  ) resulting from 54,996 *visits*, and 1,195 *visits* whose centers differ  $> 5'$  from the center of their *coadd*, affecting 640 *coadds*. These 640 *bad coadds* are made up of 2,400 *visits* in total; we discarded these *coadds*, and used only *visits* with both FUV and NUV exposure  $> 0$  to replace them: 1,468 *visits*.

## 5.2. Criteria for constructing the UV source catalog

The catalog was constructed from the database source photometry with the criteria given below, following the recipe of Bianchi et al. (2011a,b, 2014a), where other details can be found, and of which the present catalogs represent the updated and expanded version. We used the photometry from 28,067 AIS good *coadds*, plus 1,468 *visits* that replaced 635 of the 640 *bad coadds* as described in the previous section; the ensemble of these datasets includes the whole AIS coverage with both FUV and NUV detectors exposed.

The catalog includes sources:

- **from observations with both FUV and NUV detectors on.** This restriction is useful for science applications in which the fraction of sources with a given FUV-NUV color is of interest, or to estimate the fraction of sources with significant detection in FUV over the total NUV detections (e.g., Bianchi et al. (2014a), and Sections 6 and 8). More observations, taken with one of the two detectors turned off (mostly FUV), exist in the MAST database. Including in our catalog observations where one detector was not exposed would bias any statistical analysis, since the FUV magnitude

of a NUV-detected source appears in the database as a non-detection ( $FUV_{mag}=-999$ ) either because the FUV detector was turned off, or the FUV detector was on but the FUV flux of that source was actually below detection threshold. In some cases the exposure is not the same in both detectors (exposure times are also given in Table 4). We used all AIS data in which both detectors’ exposures were  $>0$ .

- **within the central  $0.55^\circ$  (GUVcat\_AIS\_055) or  $0.50^\circ$  (GUVcat\_AIS\_050) radius of the field-of-view** ( $fov\_radius \leq 0.55^\circ$  or  $0.50^\circ$ , respectively), to avoid sources with poor photometry and astrometry near the edge of the field, and rim artifacts. This restriction yields source samples with overall homogeneous quality, and minimize artifacts, without great loss of area coverage. Users interested in a particular source that falls on the outermost edge of a GALEX field should obtain the measurements from the GALEX database and carefully examine the quality. The less conservative  $fov\_radius \leq 0.55^\circ$  limit reduces gaps between fields and increases total area coverage (see Section 7), while still excluding the outermost rim in nearly all data (Section 6.2).
- **with NUV magnitude errors  $\leq 0.5\text{mag}$** ; that is, all sources with NUV detections are retained, regardless of detection in the FUV filter. Typically, about 10% of the NUV-detected sources are also detected in FUV (Bianchi et al. 2011b). Effects of error cuts on the resulting samples can be seen from Figure 4 of Bianchi et al. (2011a), and Figures 2–4 of Bianchi et al. (2011b). Sources in the database having a FUV detection with no NUV counterpart will not make it into the catalog: these cases are very rare, and are either mismatches or artifacts (see later), or cases where the pipeline resolves individual sources in FUV but merges them into one extended source in NUV, such as for example in the center of globular clusters (Fig. 5.c).
- **Unique**, i.e. duplicate measurements of the same source are identified and removed: each object is counted only once in the GUVcat catalog. The procedure for defining duplicates is fully described in Appendix A, as it involves often neglected complexities. The unique-source catalog is useful for most science applications, such as examining density of sources, and for cross-matching with other catalogs. We provide online also a master catalog (GUVcat\_plus) in which duplicate measurements are identified and flagged but not removed. Details can be found in Appendix A. The identified repeated measurements could be used in principle for serendipitous variability searches; we provide tags giving magnitude difference between “primary” and “secondary” sources, but mainly for the purpose of checking consistency between repeated measurements. Because our catalog made use of *coadds* as much as possible, variability searches will be more productive on catalogs extracted at *visit* level, or better yet with sub-*visit* integrations, which we will present in follow-up works (Bianchi et al. 2017c; Million et

al 2017).

There are five AIS fields (*photoextractid* = 6379923033125027840, 6381259965176217600, 6379711852804308992, 6372041728408420352 and 6379571150749433856) where both FUV and NUV detectors were exposed, but NUV and FUV sources do not match: all sources with NUV measurements show no FUV detection (FUV\_mag=-999), and viceversa all FUV sources have NUV\_mag=-999. These fields are nonetheless included in the catalog because they satisfy all the defined criteria, however users must keep in mind that such mismatch would cause a false statistics of FUV-NUV colors in these fields. In Appendix C we show one of these fields, and also use it as example to illustrate the main artifact flags of the GALEX sources.

## 6. Content and Structure of the Catalog

The catalog includes 82,992,086 unique sources (GUVcat\_AIS\_055), from a total of 86,632,284 AIS measurements (GUVcat\_AIS\_plus, before duplicates are removed). The version restricted to sources within the central  $1^\circ$  of the GALEX field, GUVcat\_AIS\_050, contains 69,772,677 sources. Note that the majority of these measurements are from *coadds* (Section 5.1), therefore duplicate measurements only occur in field overlaps or repetitions. These fields are the result of over 56,000 *visits*, many repeats at *visit* level were already merged in the *good coadds* we used.

Tables 6 and 7 give the number of sources included in GUVcat\_AIS, at different galactocentric latitudes, the fraction which have multiple measurements, those affected by artifacts, and samples with magnitude and color selections. Whole-sky maps of the density of UV sources and their characteristics across the sky were shown by Bianchi et al. (2014a), which highlighted interesting distributions of hot stars in the Milky Way, among other trends.

The catalog gives several tags for each source, including position (R.A., Dec., Galactic  $l, b$ ), photometry measurements in FUV and NUV and their errors (“nuv\_mag” and “fuv\_mag” are the “best” measurements as chosen by the pipeline, and preferable in most cases; other measurements are also included, such as PSF photometry, aperture photometry with different apertures, and Kron-like elliptical aperture magnitudes), other parameters useful to retrieve the original image from which the photometry was extracted (tag *photoextractid*), as well as artifact flags and extraction flags that can be used to eliminate spurious sources (see Section 6.2 below). In addition to these astrometry and photometry tags, propagated from the GALEX pipeline processing, we include new tags informative of the existence of duplicate [AIS] measurements or nearby sources (described in Appendix A), and tags in-

dicating whether the source falls within the footprint of a large object such as galaxy or Milky Way stellar cluster. These added tags facilitate extraction of clean samples for science applications of the catalog. The complete list of tags and their description is given in Appendix B.

The catalogs can be downloaded from the author’s web site: <http://dolomiti.pha.jhu.edu/uvsky/#GUVcat>, and will be also available from the MAST casjobs web site (<http://mastweb.stsci.edu/gcasjobs>) and from the SIMBAD Vizier database, which allows VO-type queries including cross-correlation with other catalogs in the same database.<sup>5</sup>

### 6.1. Sources in Extended Clusters or Galaxies

While we cannot and should not exclude from the catalog the sources (as measured by the pipeline) in extended galaxies or crowded fields, for convenience of catalog’s users we flagged all sources that fall within the footprint Galactic stellar clusters or galaxies larger than  $1'$ . We added a tag *inlargeobj* which contains the identifier of the large object prefixed by “GA:” for galaxies (e.g., GA:M33), “GC:” or “OC:” for globular clusters and open clusters respectively (e.g., GC:NGC5272), “SC:” for less well defined cluster types. We also added a tag *largeobjsize* which gives the  $D_{25}$  diameter for galaxies, or twice the radius for stellar clusters. Note that  $1'$  is a very conservative limit, for the purpose of eliminating crowded regions, but a user can choose to worry only about larger objects by using a combination of these two tags, which we highly recommend. We provide finding charts for all of the extended objects ( $>1'$ ) in the footprint of GUVcat\_AIS. These can be found in the GUVcat tools on the author’s web site <http://dolomiti.pha.jhu.edu/uvsky/#GUVcat>.

The stellar clusters included for flagging were taken from the compilation available at <https://heasarc.gsfc.nasa.gov/W3Browse/all/mwsc.htm>, which basically includes all globular clusters from Harris (1996), which are all confirmed objects, and includes as “open clusters” confirmed, candidate or doubtful clusters, or spurious objects such as OB associations and large nebulae. Of course the definition of open clusters is less specific than is possible for globular clusters, and their stellar density also varies more widely. As pointed out in Section 4.2, only in the most crowded regions of clusters the source extraction would fail. In the dense central regions of globular clusters, the pipeline sometimes integrates a

---

<sup>5</sup> The earlier version of these catalogs (with less data coverage and fewer parameters) is accessible with Vizier at: <http://vizier.u-strasbg.fr/viz-bin/VizieR-3?-source=II/312>, and from MAST at: [http://archive.stsci.edu/prepds/bianchi\\_gr5xdr/](http://archive.stsci.edu/prepds/bianchi_gr5xdr/).

large area as one extended source. This may happen both for galaxies and for crowded stellar clusters: examples are shown in Figure 5.

The *heasarc* catalog gives three values of radius:  $r_o$  (radius of the cluster core in the visible, corresponding to the distance from the center where the radial density profile becomes flatter),  $r_1$  (where the radial density profile abruptly stops decreasing) and  $r_2$  (where the surface density of stars equals the average density of the surrounding field); it also gives the number of (optical) sources within these radii. In order to select the most appropriate value of cluster radius for our purpose, i.e. to exclude only sources which would very likely introduce statistical biases, we examined two classical examples, NGC188 and NGC2420. By combining the number of sources with the cluster sizes, we concluded that  $r_1$  is a good compromise, although somewhat conservative. OB associations are interesting objects *per se*, but are sparse and are much less likely to suffer from crowding problems, and to introduce significant overdensities in global source counts. Therefore, we restrict the ‘open cluster’ list to only *confirmed* clusters, and we further restricted these by combining the criteria of *cluster\_status* not “C” (candidate) and *cluster\_type* neither “DUB” nor “NON”. In total, 48 GC and 324 OC are included, entirely or partly, in the GUVcat footprint, all are shown in our *uvsky* web pages. Table 2 (electronic only) lists centers, size and other parameters for Galactic clusters.

Table 3 (electronic only) gives a list of centers, major and minor axis and position angle (p.a.) and other basic parameters for extended galaxies with major axis  $D_{25} \geq 1'$ . The galaxies (22,037) were selected from the hyperleda database, with no other restriction than the size,  $D_{25} \geq 1'$ . In total, 15,659 of these galaxies with  $D_{25} \geq 1'$  are included (at least partly) in the GUVcat\_AIS footprint. We flagged sources out to  $1.25 \times D_{25}$ , a choice based on inspection of several maps, available on our web site<sup>6</sup>, of which Figure 5 shows an example. Note that most galaxies with size  $\approx 1'$  are probably detected as a single (extended) source, or a few sources, in the GALEX data. Therefore, while the  $1'$  size limit provides a very comprehensive flagging, for statistical analyses of large samples of sources a much larger radius can be used to exclude only galaxies for which the pipeline photometry is misleading.

For many science applications, such as statistical studies of source densities and luminosity functions, the area covered by the catalog must be calculated. Portions optionally excluded (because in the footprint of a cluster or galaxy) must be taken into account in the area calculation. Our interactive area calculation tools will offer some options (Section 7) for area estimate in the cases where large object footprints are excluded from the samples. We stress that, when catalogs over large areas are used, removing very small footprints may

---

<sup>6</sup><http://dolomiti.pha.jhu.edu/uvsky/#GUVcat>

introduce additional un-necessary uncertainties in area calculations, depending on the tessellation steps of the sky grid used for area calculation relative to size of the areas being excluded. More details are provided with the area calculation tools (Bianchi & de la Vega 2017).

## 6.2. Flagged artifacts

Table 2 of the GALEX GR6 documentation ([galex.stsci.edu/GR6/?page=ddfaq#6](http://galex.stsci.edu/GR6/?page=ddfaq#6)) lists the value of the *artifact* flags (*FUV\_artifact* and *NUV\_artifact* in the catalog), and suggests that the only artifact flags causing real concern are the *Dichroic reflection* (*artifact*=4, base 10 value, or *artifact*=64 when a *coadd* has enough *visits* at different position angles that masking the Dichroic reflection does not decrease the flux by more than 1/3rd) and *Window reflection* (applicable to the NUV detector only: *NUV\_artifact*=2). Most of the artifacts in the original database are caused by the detector rim (*artifact*=32), or reflections around the edge: these do not affect our catalog since we exclude the outer edge of the field of view (Figure 8). In more detail: the version which retains sources within  $0.55^\circ$  from the field centers, GUVcat\_AIS\_055, excludes a  $0.06^\circ$ -wide outer ring; this is sufficient to eliminate rim artifacts, except in a few cases because in GUVcat we retained *coadds* of *visits* with a tolerance of up to  $5'$  between the pointings of the individual *visits*. In the worse case of two coadded *visits* having centers  $5'$  apart, the *fov\_radius* of the *coadd* sources may also differ by up to  $5'$  from the actual distance of the source from the center of its *visit*, therefore a few rim artifacts may be included. Such tolerance of  $5'$  centring difference between *visits* of *coadds* was chosen to maximize the area coverage of the catalog, and to avoid throwing away much data or much exposure depth. As a consequence, in GUVcat\_AIS\_055 there remain 23,218 sources with either FUV or NUV rim artifact flag set, out of the  $\sim 93$  million catalog sources. These sources have *fov\_radius* (distance from the *coadd* center) between  $0.5125$  and  $0.55^\circ$ , and all come from *coadds* as expected. By comparison, there are 31,184,260 sources with either *fuv\_artifact* or *nuv\_artifact* rim flag set (6,765,612 with *fuv\_artifact* flag set) in the whole *visitphotoobjall* GALEX database, and 25,259,384 sources with *fuv\_artifact* or *nuv\_artifact* rim flag set (25,221,382 NUV; 18,592,421 FUV) in the whole *photoobjall* GALEX database of 292,296,119 entries. Note that the GALEX field has a diameter of  $\approx 1.2^\circ$ , therefore the actual *fov\_radius* of any source should always be  $\leq 0.6^\circ$ , and rim sources should have *fov\_radius*  $\sim 0.6$ , but in the MAST GALEX database the sources with “rim” artifact flag set have values of *fov\_radius* between 0 and  $> 1^\circ$ , an effect of the improper *coadd* described in Section 5.1, where the rim artifact has been propagated from the *visit*-level processing, while *fov\_radius* has been recalculated using the center of the *coadd*, therefore an actual rim source may end up having apparent *fov\_radius* near zero

(near the center of the *coadd*) or a value almost twice the GALEX f.o.v. radius. This is illustrated in Figure 3 and was explained in Section 5.1. This problem is cured in GUVcat.

In the GUVcat\_AIS\_050 catalog there are no rim or edge artifacts, since we only retained sources within  $0.5^\circ$  from the field center, which leaves out, even with a  $5'$  tolerance for *coadds*, an outer ring of  $\geq 0.1^\circ$  width. This restriction comes at the price of a  $\sim 10.7\%$  decrease in area coverage, as explained in Section 7, introducing occasional gaps between adjacent fields.

Masked variable pixels (*artifact*=128) and masked detector hotspots (*artifact*=256) may degrade the quality of a photometric measurement but would not introduce spurious sources, and they are rare, therefore they are not relevant for the purpose of source counts. What does introduce a high number of spurious source detections (once the rim is excluded) are reflections and 'ghosts' near very bright sources. We show examples in Appendix C. A conservative recommendation is to eliminate sources with *artifact*=4 or 2. Note that if more than one artifact is deemed to be present, the flag value is the sum of all the artifacts affecting the source. Table 6 gives also the fraction of sources with different artifact flags in the GUVcat\_AIS catalog, and report the artifact definitions in the table's footnote.

## 7. Area Coverage of the Catalogs

For studies involving density of sources (number per unit area), the exact area coverage of the catalog must be known. As we removed duplicate measurements of the same source, we must calculate the area covered by the surveys accounting for overlaps. We must also account for possible gaps between fields; these may occur because of the tiling strategy (for example, to avoid bright stars that would damage the detectors), or because the actual pointing of an observation is slightly off from the planned position, and because we limited our catalogs to sources within the central  $1.1^\circ$  (or  $1.0^\circ$ ) diameter of the GALEX field.

We calculated the total actual area covered by GUVcat\_AIS with the method of Bianchi et al. (2011a): we divided the sky in small tesserae, and added the areas of all tesserae which fall within  $0.55^\circ$  (or  $0.50^\circ$ ) from the center of every field used in the catalog, ensuring that each tessera is counted only once. The total area covered is 24,790 square degrees for GUVcat\_AIS\_055, and 22,125 square degrees for GUVcat\_AIS\_050. This area of “unique-coverage” is  $\approx 95\%$  (with *fov\_radius* $\leq 0.55$ ) and  $88\%$  (with *fov\_radius* $\leq 0.5$ ) of the sum of areas of the fields used (if there was no overlap between observations), implying an overall overlap of  $\approx 11.7\%$  and  $4.6\%$  respectively among the AIS fields used. Area coverage of 5-degrees latitude slices for the catalog are given in Table 6.

Because both gaps and overlaps between fields occur, the actual area coverage must be computed for each region of the sky where one desires to extract a sample, if the density of sources has to be estimated. An online interactive tool will be presented elsewhere, for area calculations of custom-chosen regions, for the GUVcat and BSCcat catalogs, and for matched GUVcat–optical catalogs (Bianchi & de la Vega 2017).

## 8. Conclusions and Summary

### 8.1. The UV sources across the sky

Bianchi et al. (2014a) published several maps showing the distributions of UV sources in the sky, for both the AIS and the deeper MIS survey. In Figure 6 we show the density of sources (number per square degree) detected in the NUV and FUV bands; as discussed extensively by Bianchi et al. (2011a,b, 2014a) the number of FUV detections is typically ten times less than the NUV detections overall; this happens because hot stars, and blue galaxies, are much more rare than cooler (redder) objects. More specifically, the fraction depends on Galactic latitude and on the magnitude depth considered, because the number of extragalactic sources with respect to Galactic stars increases rapidly towards fainter magnitudes. The relative fractions are a combinations of the intrinsic distribution of different types of sources, whereby the density of Galactic stars increases towards the disk of the Milky Way, while the distribution of extragalactic sources does not depend on the Milky Way structure, but all sources are affected by the Milky Way dust, which is mostly confined to a thin disk. The reddening depends therefore on the line of sight towards the sources going through more or less of the dust disk. This effect was dramatically illustrated by Figure 2 (bottom) of Bianchi et al. (2011a): the “V-shape” region devoided of UV-source counts in their figure is essentially a direct image of the dust disk. It is also visible, though less evident, in Figure 6.

In Figure 6 we plot the density of NUV and of FUV sources in GUVcat\_AIS (top plot), as a whole and divided by NUV magnitude ranges: the plots show that the sources fainter than  $\text{NUV\_mag}=21\text{mag}$  dominate the sample, in spite the AIS is the shallowest survey, and especially so in the NUV where extra-galactic objects are more prominent. The bottom panels show the fraction of FUV detections over NUV detections, again as a function of Galactic latitude, and among these, the hot and very hot sources ( $\text{FUV\_mag-NUV\_mag} \leq 0.5$  and  $\leq 0.0$  respectively). Such UV color cuts correspond to different stellar  $T_{\text{eff}}$  for different types of stars (Bianchi 2009), but roughly hotter than  $\sim 15,000\text{K}$ . Some QSOs may intrude these FUV-NUV color cuts, as shown by Bianchi et al. (2009): these affect the faint sources most. The different behaviour of relative source densities in Figure 6 reflects the fact

that brighter samples (and hotter samples) are dominated by Galactic stars, which are more numerous in the Milky Way disk (see e.g., Bianchi et al. (2011a)).

## 8.2. Summary of Suggestions and Caveats for Using the Catalog

To conclude, we distill here, in terms of practical advice for users, the relevant information on the catalogs presented in this paper.

- **GUVcat\_AIS contains unique measurements** of all sources from AIS observations with both FUV and NUV detectors exposed. Duplicates measurements are removed in the main catalog, however a version GUVcat\_AISplus is accessible where duplicate measurements are flagged but not removed.
- **GUVcat is available** from <http://dolomiti.pha.jhu.edu/uvsky/#GUVcat> as well as MAST casjobs (<http://mastweb.stsci.edu/gcasjobs>), and SIMBAD Vizier.
- **Sources near the field’s edge** have been excluded, because they are mostly artifacts and have poor photometry. GUVcat\_AIS\_0.55 contains sources within  $0.55^\circ$  of the field’s center, GUVcat\_AIS\_0.50 only sources within  $0.50^\circ$ . The first has a larger area coverage, fewer gaps, at the expense of a few rim artifacts intruding the catalog, these must be sieved from samples by using the `artifact=32` flag (Section 6.2). Tables 6 and 7 give statistical information on the number of sources, and the fraction of sources affected by artifacts, or in given UV-color ranges, in total and divided by Galactic latitude.
- **area coverage** of our catalog GUVcat, BCScat, and of overlap of these catalogs with optical databases, can be calculated for any desired region of the sky with the tool of Bianchi & de la Vega (2017). See also Column 9 of Table 6.
- **Extended Objects:** beware of sources in the footprint of large galaxies or crowded stellar clusters (Section 6.1). These can be identified and eliminated with the two tags *inlargeobj* and *largeobjsize*, provided in GUVcat. The web site <http://dolomiti.pha.jhu.edu/#GUVcat> gives also finding charts and information on all large objects included entirely or partly in GUVcat.

The size limit of the extended objects that one should eliminate from the catalog depends on the specific objectives and sample size; if one needs to compute area coverage of the extracted sample, the excluded footprints can be accounted for with our area calculation tool (Bianchi & de la Vega 2017), however the interactive public version

currently uses a sky tessellation with a grid step of  $0.1^\circ$  (so that a computation over the whole sky can be accomplished in a few tens seconds); excluding any area smaller than, or comparable to the grid tesserae will introduce uncertainties in the area estimate.

- **Magellanic Clouds:** only the periphery of the Magellanic Clouds is included in GUVcat, because the central regions are only observed in NUV. Even the peripheral fields are crowded enough to pose a challenge to the pipeline photometric procedures: for point sources within a  $15^\circ$  radial distance from the center of the LMC, and a  $10^\circ$  radial distance from the SMC, it is preferable to use the custom-made catalog of Thilker et al. (2017) and to avoid using this catalog or the master database. In Table 7 we count sources within  $15^\circ / 10^\circ$  radial distance from LMC / SMC, but for consistency with other galaxies, the flag *inlargeobj* is set only for GUVcat sources within  $1.25 \times$  the Hyperleda  $D_{25}$  size, which is much smaller; these sources have flag GA:ESO056-115 and GA:NGC0292 for LMC and SMC respectively. For the statistical overview in Figure 6 we conservatively excluded the  $15^\circ / 10^\circ$  degree areas, since we noted an overdensity of sources even in the outermost periphery of the Clouds.
- **Reddening correction:** Table 1 gives extinction coefficients in the GALEX FUV and NUV bands for representative known types of interstellar dust; these coefficients can be used to correct the UV magnitudes for reddening. In the GUVcat catalog, an  $E_{B-V}$  value is given for each source, based on the extinction maps of Schlegel et al. (1998); this value is approximate as it represents an interpolation from low-resolution maps at the source position, and as such it is also an upper limit (a Galactic source very close will only suffer the absorption by the local component of the dust along the line of sight), anyway it is a convenient indication of reddening. As noted by Bianchi et al. (2011a,b); Bianchi (2011), the GALEX FUV-NUV color is almost reddening-free, for Milky-Way typical dust (see also Table 1), and therefore it could be used to select hot stellar sources, almost independently of reddening, by Bianchi et al. (2011a).

### 8.3. Is a source not detected, or not observed?

When one matches a source list to the GALEX catalog, if a source is not found (either in the entire database, or in GUVcat\_AIS, or in any other catalog), one needs to know whether the source was observed but too faint to be detected in a given filter, or it was not in the footprint of any actual observation. This holds for GALEX, SDSS, and any database which does not have a complete coverage of the sky, due to the nature of the survey or because there are some gaps or unusable portions of data.

The easiest and safest way to find out whether a given celestial position is within the footprint of any GALEX observation is to match the source coordinates to the list of *visit* centers (*visitphotoextract* in MAST casjob ) and check if the source position is within the f.o.v. radius from the center of any observation (*navaspra*, *navaspde* for NUV; *favaspra*, *favaspde* for FUV; *avaspra*, *favaspdec* for the combined FUV+NUV source list). This test should be done at *visit* level, because of the issue of *bad coadds* described in Section 5.1. For the “good *coadds*” (only) one could use the *photoextract* values.

For other surveys, such as for example SDSS, where gaps among fields or failed observations are not always mapped consistently into the footprint tool (e.g., Bianchi et al. (2011a)), one has to search for sources in a wider area around the source of interest, and if other sources are found around the position, a negative detection for the source of interest will imply that the source was observed but its flux is below detection threshold. In this case, one could derive an upper limit from the exposure time of the observations in the area. This procedure works in any case, but it is more cumbersome, and it may not be entirely safe: if the catalog sources are sparse, one would need to probe fairly large portions of sky around the source of interest, to avoid false negatives, but in this way a ‘positive’ detection will mean that some wide area around the desired position has some sources: if that happens to be near a field edge and the desired position is just outside the edge, the “poor resolution” sampling of the surroundings may give a false positive.

We are very grateful to Imant Platais for helpful suggestions concerning the selection of stellar cluster parameters, to Chase Million for always providing expert advice on GALEX data issues and clarifications on the GALEX pipeline, and to Scott Fleming for useful discussions on GALEX science projects. This work was supported by NASA ADAP grant NNX14AF88G. We made use of the GALEX database in the MAST archive, which is funded by the NASA Office of Space Science.

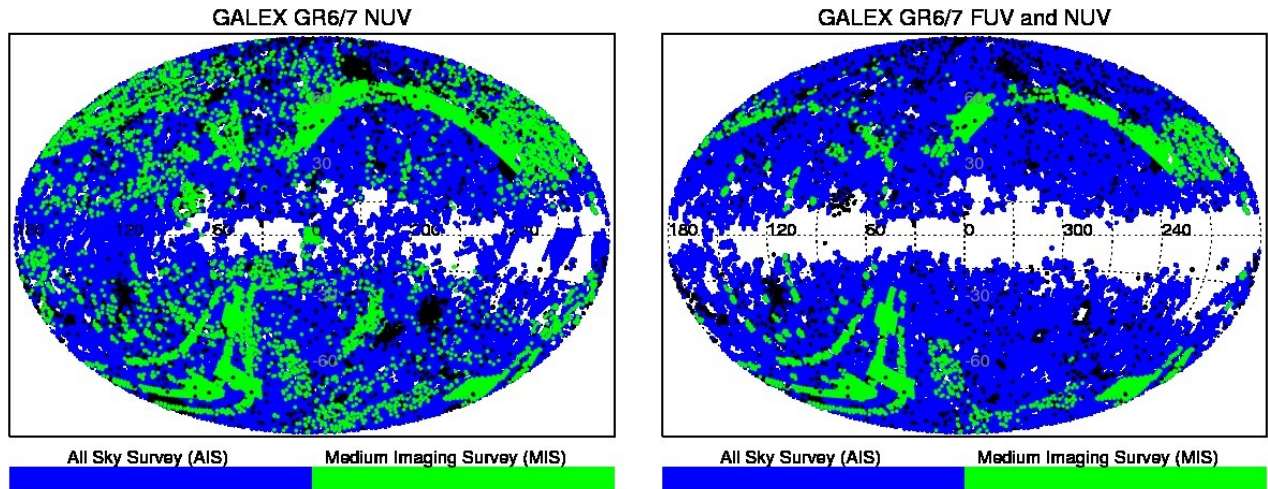


Fig. 1.— Sky coverage, in Galactic coordinates, of the GALEX imaging (GR6plus7 data release). The surveys with the largest area coverage are AIS (shown in blue) and MIS (shown in green). Observations from other surveys are shown in black (figure adapted from Bianchi et al. 2014a). Data from the trailed CAUSE observations at the end of the mission are not shown. Left: fields observed with the NUV detector on, regardless of FUV-detector status; right: fields observed with both FUV and NUV detectors on. The latter constitute the present catalog.

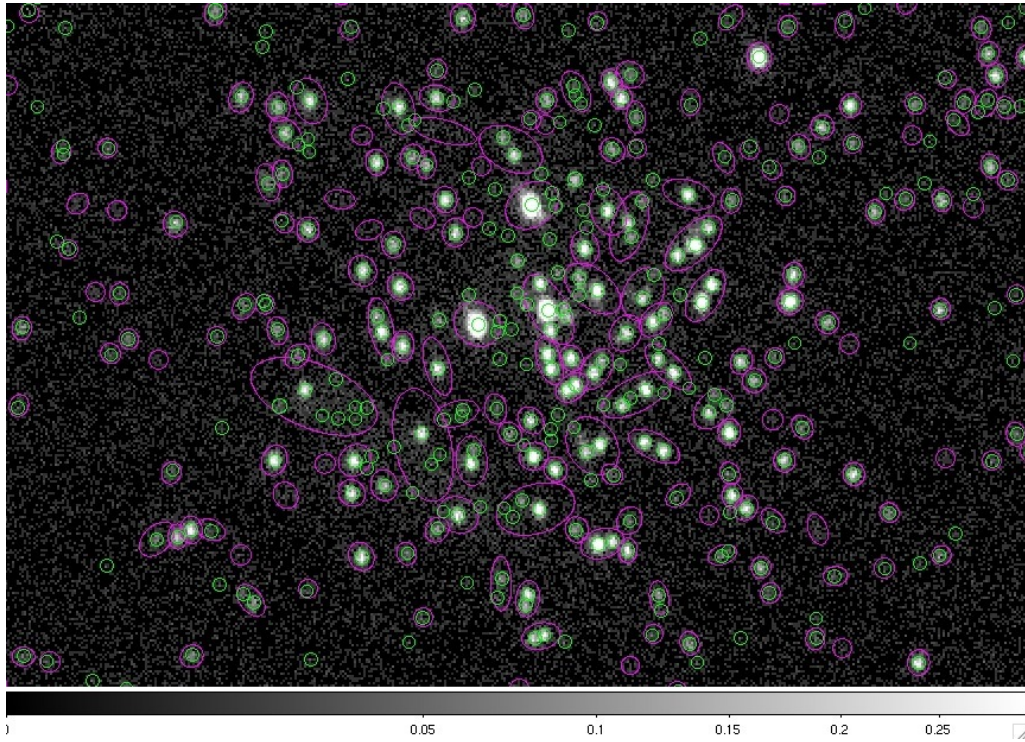


Fig. 2.— A portion of the Galactic open cluster NGC 2420 imaged by GALEX; detected sources as defined by the standard pipeline are outlined in pink, and from our custom-made photometry (de Martino et al. 2008) in green. The example illustrates the case of some crowded pointlike sources being merged by the pipeline into one extended source. In the outskirts of the cluster, less crowded, the pipeline source identification matches ours very well.

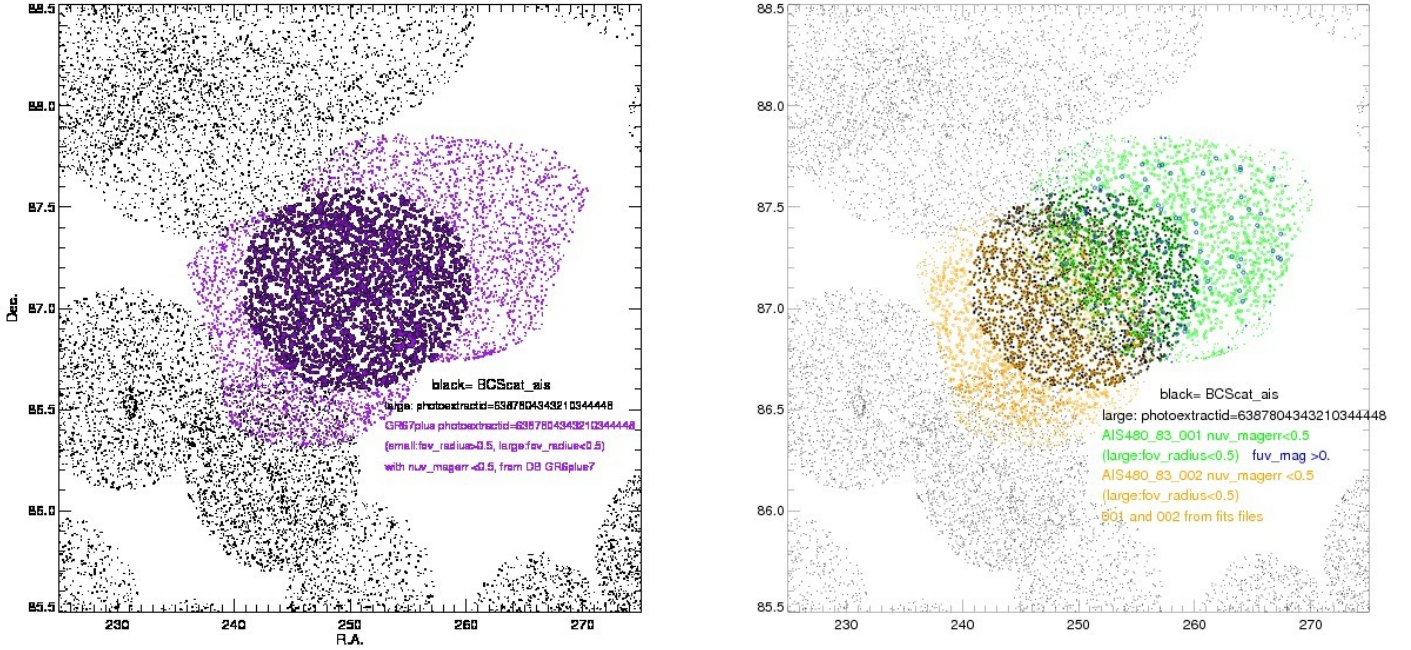


Fig. 3.— **To be printed in landscape** *Left*: database sources included in *tile* AIS\_480 are shown as purple dots. They result from merging two *visits* (right); the large black dots are sources within  $0.5^\circ$  from the center of the *coadd*, thus in principle meeting the criterion for our catalog (and BCScat). Smaller black dots are sources in nearby fields. *Right*: Over the pipeline-merged sources with  $fov\_radius < 0.5^\circ$  (black dots), the *visit*-level sources are shown in dark yellow (*visit* with NUV exposure only) and green (*visit* with both NUV and FUV exposures). On the latter, blue circles mark sources with significant detection also in FUV. We use large/small symbols to indicate sources inside/outside of a  $0.5^\circ$  radius from the actual center of each *visit*. In the database *coadd* all purple sources are given exposure times equal to the sum of the two *visits*, but this is correct only for those in the small intersection of yellow and green dots. Also, sources from the rim of both *visits* appear to have a small distance from the *coadd* center, because the pipeline assigned a value of  $fov\_radius$  based on the *coadd* center, rather than on the center of the parent observation, and therefore these rim sources will not be discarded by a selection in  $fov\_radius$ .

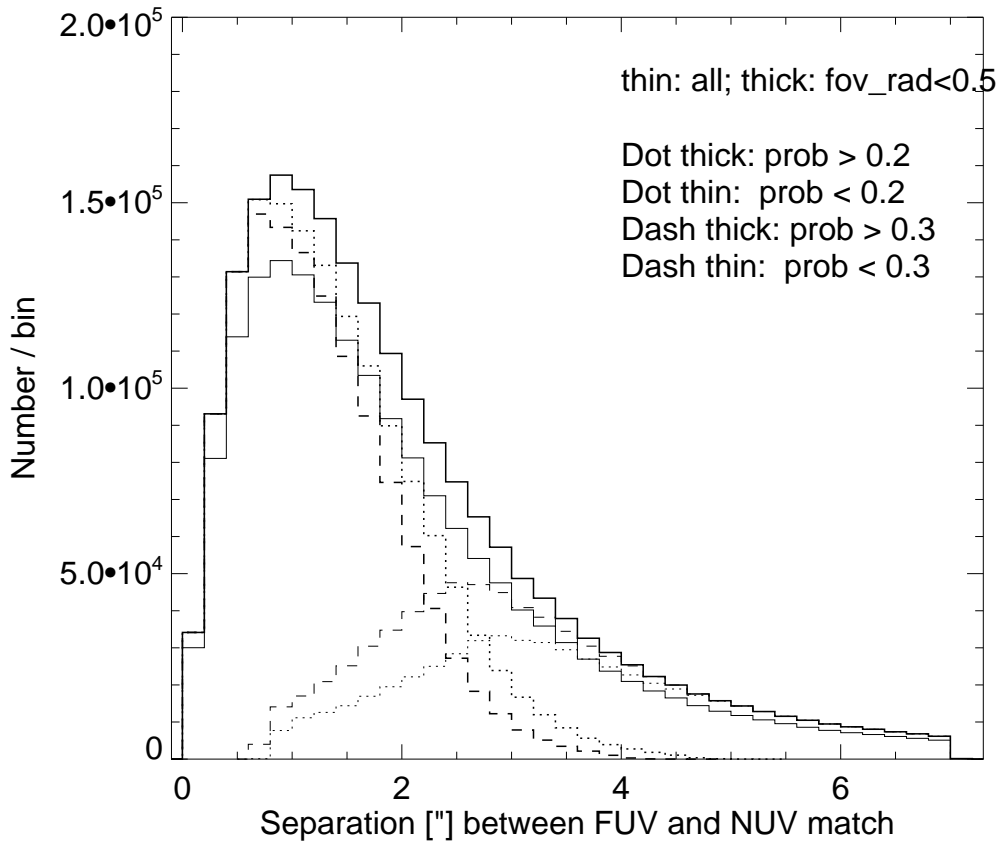


Fig. 4.— Distribution of the separation between FUV and NUV position of the sources in the GALEX database. A representative sample of 2 million sources is shown. Subsamples with cuts in the tag *probability* [that the match is real] are shown.

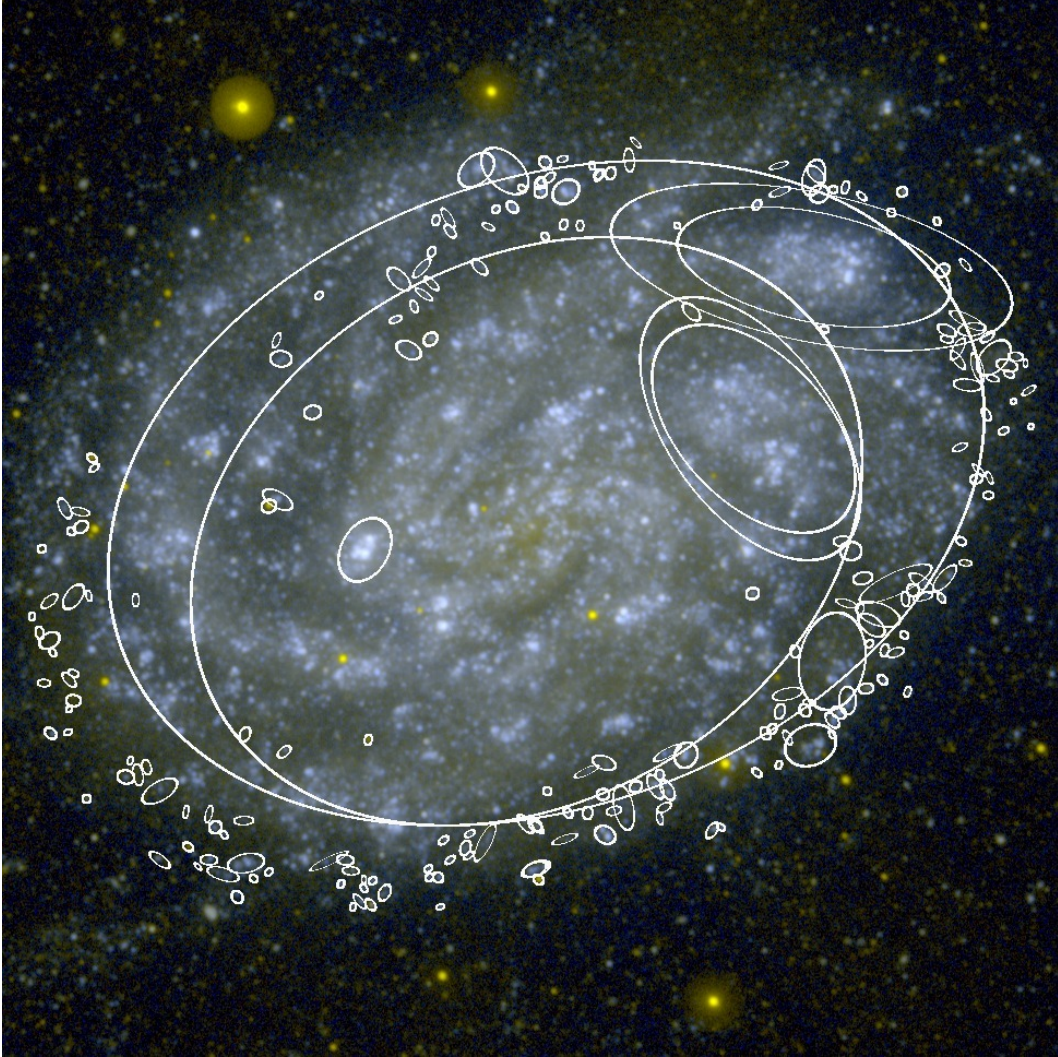


Fig. 5.— Example of pipeline photometry for an extended disk galaxy, NGC300 ( $D_{25} \approx 0.2^\circ$ ). The central parts of the disk are measured by the pipeline as unresolved extended sources; in the periphery and less dense regions, where individual peaks are resolved, source density is much higher than in the surrounding field. Therefore, density counts of foreground stars or background AGNs for example will be highly biased if sources in this region were not excluded. We marked all sources retained in GUVcat (duplicate measurements are removed) and associated to NGC 300 by our *inlargeobj* flag (within  $1.25X D_{25}$ ). The source shape is drawn, with an ellipse based on the pipeline-derived  $2.35 \times nuv\_a\_world$ ,  $2.35 \times nuv\_b\_world$  (this choice is to match the pipeline *.ds9reg* file), *nuv\_theta* (position angle). They may appear different using  $kron\_radius \times nuv\_a\_world$ , which would show the area where the *mag\_auto* are integrated. Aside from details and differences among various magnitude extraction options, which can be examined in the catalog, the figure illustrates convincingly that pipeline photometry in very extended galaxies must not be used for source counts. The GUVcat tag *inlargeobj* allows sources in these areas to be excluded. Note that some large sources have two measurements: these come from two overlapping AIS observations, that placed the centers of the big ellipses more than  $2.5''$  apart from each other, therefore they were not eliminated as duplicates in GUVcat. The image is  $1455''$  on a side.

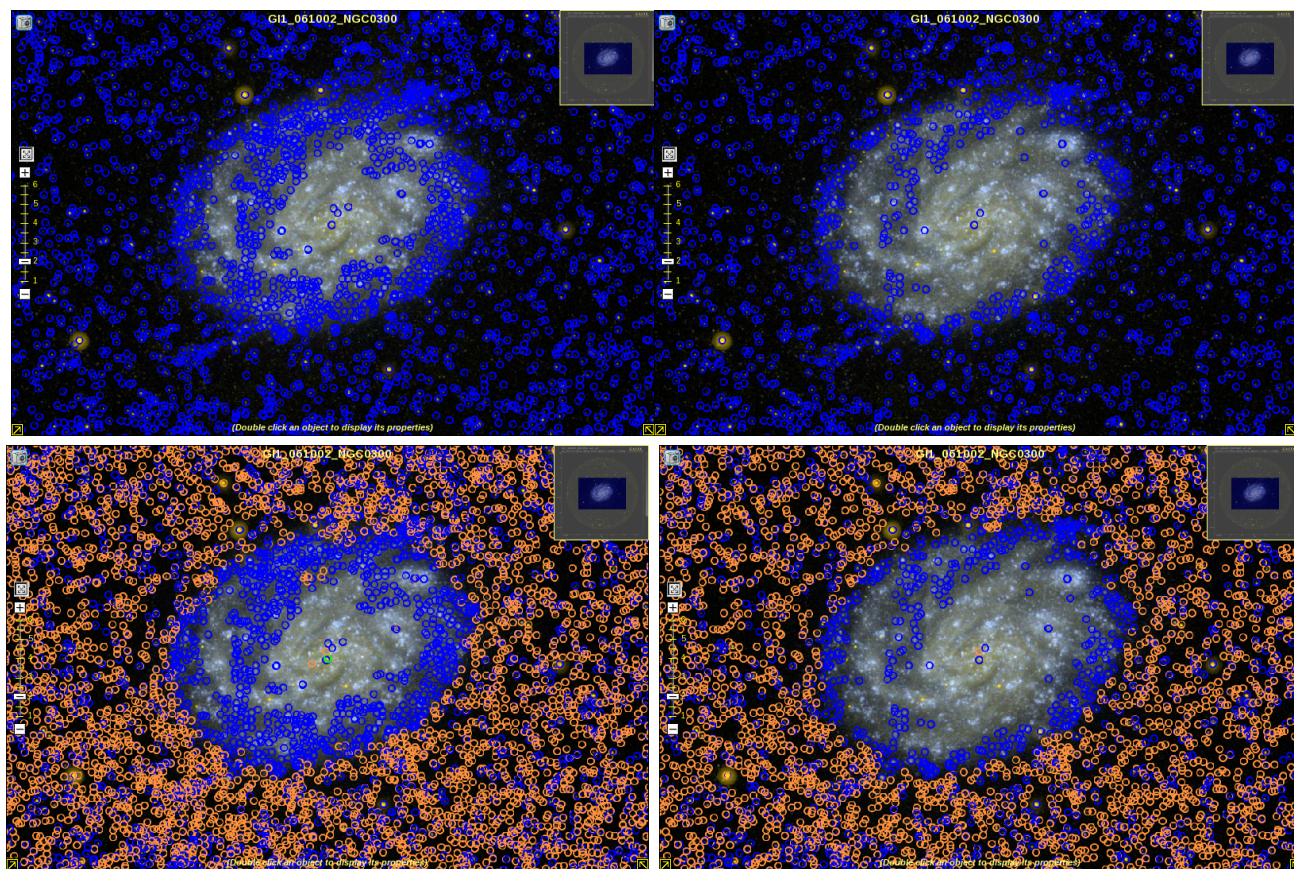


Fig. 5 (Cont.).— GALEX pipeline sources in the master database around NGC300: AIS as blue circles, NGS (about two mag deeper than AIS, see Bianchi (2009)) as orange circles. Note that here duplicates have not been removed, all measurements are shown, making the sources appear more numerous than in GUVcat (previous figure). There is an even deeper GI observation, not shown for clarity. The left panels show all entries in the master database, the right panels only those with  $NUV\_err \leq 0.5$  (as in GUVcat, which eliminates some spurious sources and many artifacts).

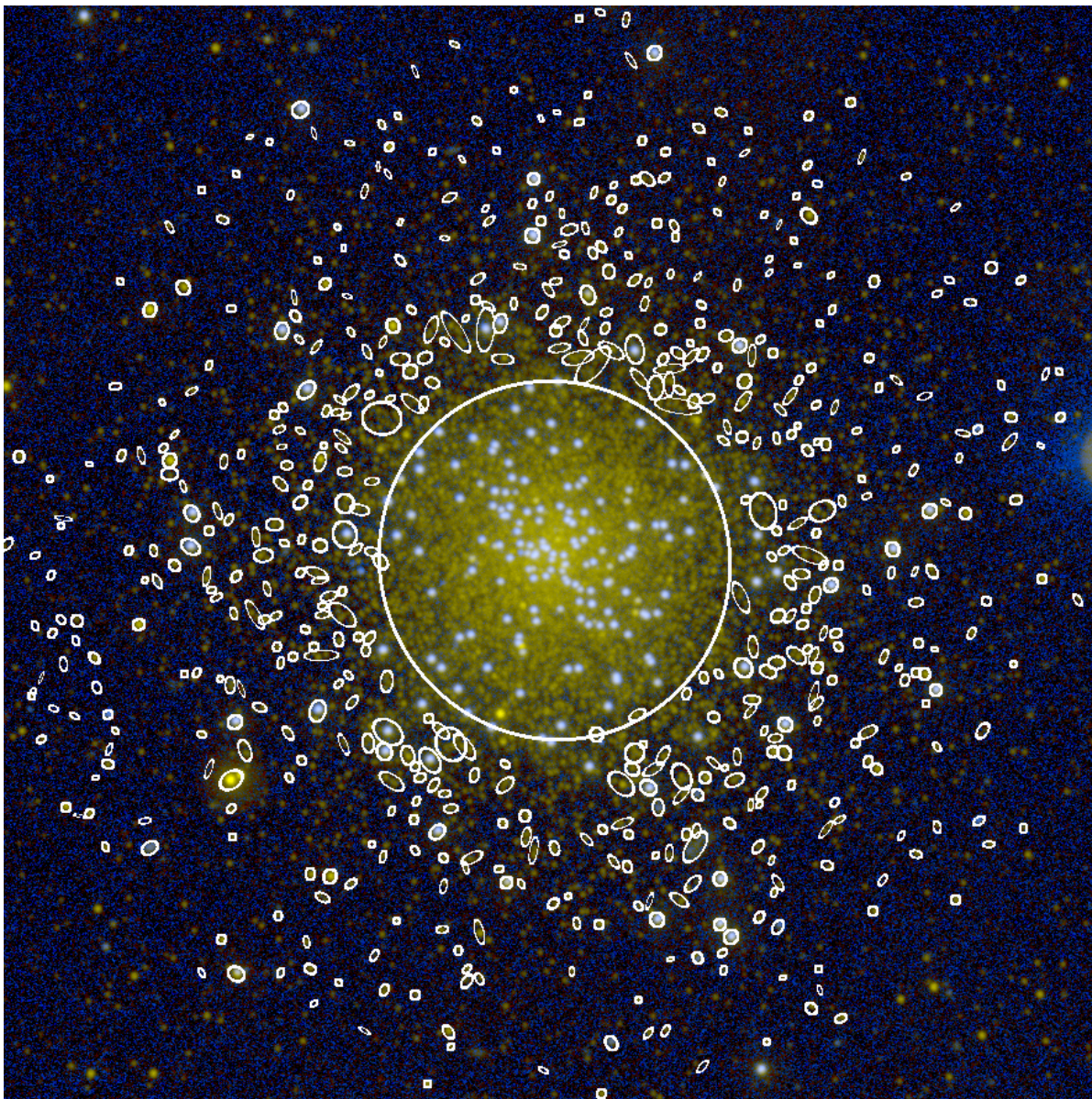


Fig. 5 (Cont.).— Example of pipeline photometry for a crowded stellar cluster, NGC6218. Sources retained in GUVcat are drawn, as in the Figure 5a, according to their database photometry extraction parameters. The color image was constructed for all available imaging for the field, including deeper exposures. Clearly visible blue sources in the cluster are only detected by the pipeline in FUV (therefore not retained in GUVcat, which uses as starting point the NUV-source detections), see next figure. The large circle is showing the pipeline aperture of the central source (drawn as explained in the previous figure), taken from NUV, showing how the pipeline neither provides accurate integrated measurements nor robust crowded-field measurements of resolved stars in the cluster. The image is  $1332''$  on a side.

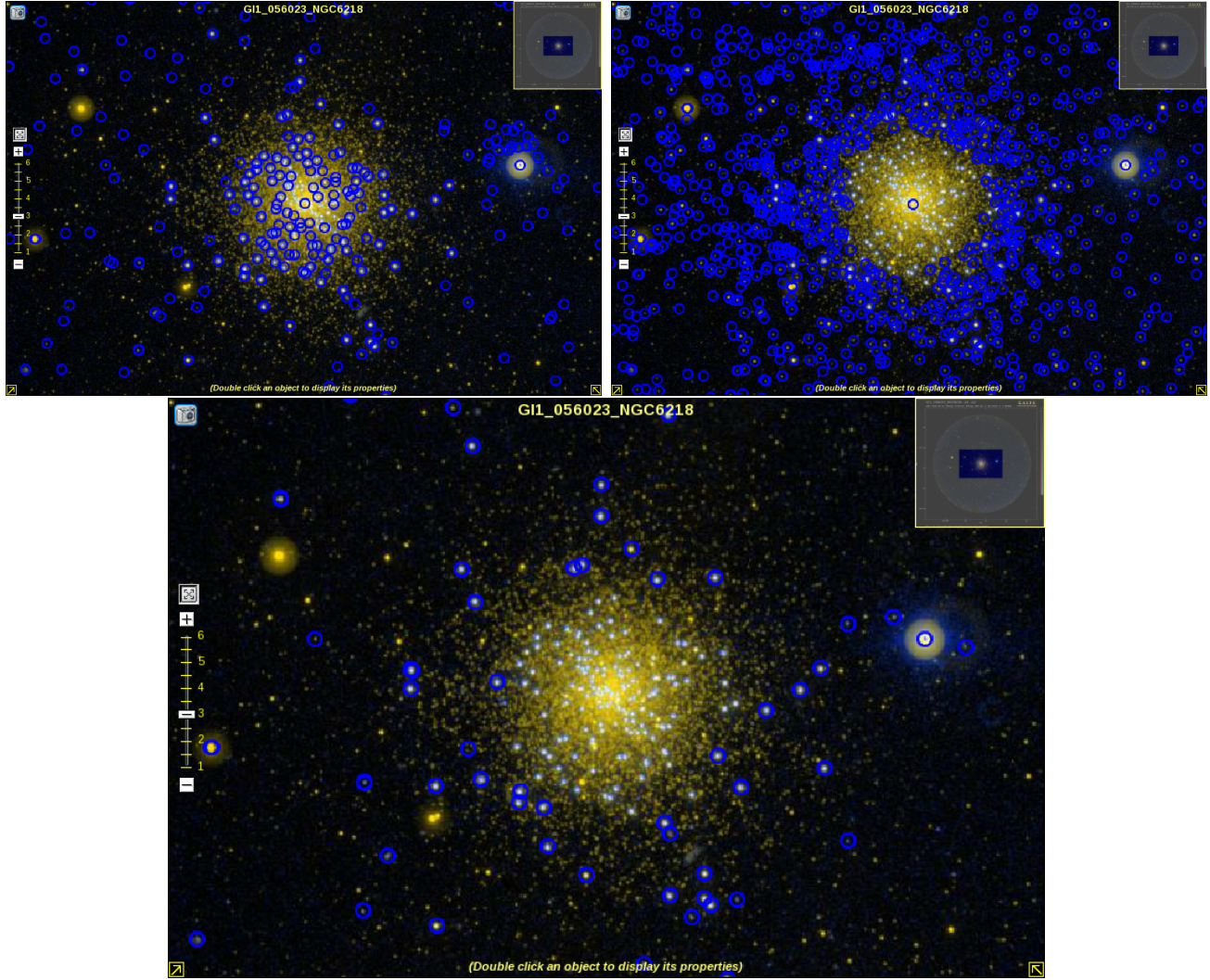


Fig. 5 (Cont.).— AIS detections in the master database for NGC 6218 (only source centers shown, not source shapes). Top: FUV detections (left) and NUV detection (right); bottom: sources detected in both FUV and NUV. Note, from the shape of the pipeline sources shown in the previous figure, that matching FUV and NUV colors in the central region would not be correct, even for sources where a match exists.

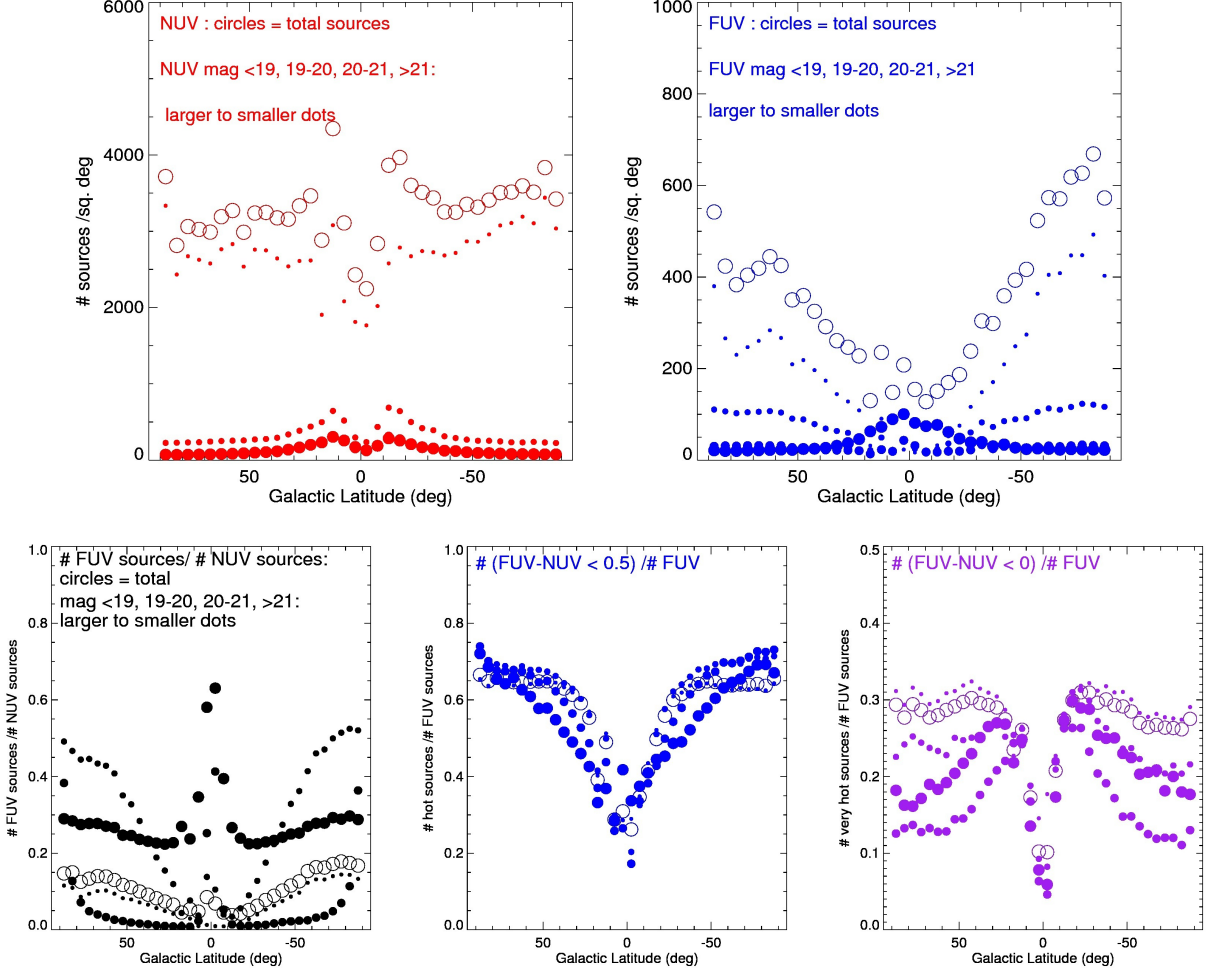


Fig. 6.— *Top:* number of sources per square degree detected in NUV (left) and in FUV (right), as a whole (circles) or by magnitude ranges (dots). Values are shown for every 5-degree latitude strip. *Bottom:* Fraction of FUV detections over NUV detections (left), fraction of sources with FUV-NUV < 0.5 (middle) and < 0.0 (right) among the FUV detections (no error cuts, but sources in the footprint of extended objects have been excluded from the counts). While the faint sources (largely extragalactic) dominate the total samples, the FUV-detected sources are mostly bright stars. We recall that, for average Galactic dust, the UV extinction is similar in FUV and NUV, and much higher in both bands than at optical wavelengths (Table 1 and Bianchi (2011)).

## REFERENCES

- Bianchi, L. & de la Vega, A. 2017, in preparation
- Bianchi, L., et al. 2017, in preparation
- Bianchi, L., Shiao, B., et al. in preparation
- Bianchi, L., Million, C. Shiao, B., et al. in preparation
- Bianchi, L. 2016, in “From the Realm of the Nebulae to the Populations of Galaxies”, eds d’Onofrio, Rampazzo & Zaggia, SPRINGER Astrophys. and Space Sci. Library N. 435, p.52
- Bianchi, L. 2014, Ap&SS, 354, 103; DOI: 10.1007/s10509-014-1935-6
- Bianchi, L., Conti, A. and Shiao, B. 2014, J. Adv. Space Res., 53, 900 ; DOI:10.1016/j.asr.2013.07.045 ; astro-ph 1312.3281 [BCScat]
- Bianchi, L. et al. 2014, J. Adv. Space Res., 53, 928; DOI: 10.1016/j.asr.2013.08.024
- Bianchi, L. 2011, Ap&SS, 335, 51; DOI: 10.1007/s10509-011-0612-2
- Bianchi, L., et al. 2011a, MNRAS, 411, 2770
- Bianchi, L., et al. 2011b, Ap&SS, 335, 161
- Bianchi, L., et al. 2011c, Ap&SS, 335, 249; DOI: 10.1007/s10509-011-0697-7
- Bianchi, L. 2009, Ap&SS, 320, 11
- Bianchi, L., Hutchings, J.B., Efremova, B., et al. 2009, AJ, 137, 3761
- Bianchi, L., Rodriguez-Merino, L., Viton, M., et al. 2007, ApJS, 173, 659
- Bianchi, L., et al. 2005, ApJ, 619, L17
- Bianchi, L., et al. 2001, AJ, 121, 2020
- Bohlin, R.C. 2001, AJ, 122, 2118
- Camarota, L., & Holberg, J.B. 2014, MNRAS, 438, 3111
- Cardelli, J.A. et al. 1989, ApJ, 345, 245

- Conti, A., Bianchi, L., Chopra, N., et al. 2014, *J.ASR*, 53, 967; DOI: 10.1016/j.asr.2013.07.022
- de la Vega, A. & Bianchi, L 2017, in preparation
- de Martino, C., Bianchi, L., Pagano, I., et al. 2008, *Mem. Soc.Astronomica Italiana*, Vol. 79, p. 704; arXiv:0712.0755
- Efremova, B., et al. 2011, *ApJ*, 730, 88
- Gil de Paz, A., et al. 2007, *ApJS*, 173, 185
- Gordon, K. & Clayton, G. 1998, *ApJ*, 500, 816
- Harris, W. E., 1996, *AJ*, 112, 1487 (edition 2010)
- Hutchings, J.B., & Bianchi, L. 2010a, *AJ*, 140, 1987
- Hutchings, J.B., & Bianchi, L. 2010b, *AJ*, 139, 630
- Kang, Y.-B., Bianchi, L., Rey, S.-C. 2009, *ApJ*, 703, 614
- Martin,D.C., et al. 2005, *ApJ*, 619, L1
- Million, C. et al. 2017, in preparation
- Misselt,K.A. et al. 1999, *ApJ*, 515, 128
- Morrissey, P., Conrow, T., Barlow, T., et al. 2007, *ApJS*, 173, 682
- Schlegel, D. J., et al 1998, *ApJ*, 500, 525
- Simons, R., Thilker, D., & Bianchi, L., et al.: 2014, *J.ASR*, 53, 939 DOI: 10.1016/j.asr.2013.07.016; arXiv: 1401.7286
- Smith, M., Bianchi, L., Shiao, B. 2014, *AJ*, 147, 159
- Thilker, D., et al. 2017, *ApJ*, in preparation
- Thilker, D., et al. 2007, *ApJ*173, 572

Table 1: Broad-band reddening corrections for different types of interstellar dust

	Type of selective extinction <sup>a</sup>			
	MW	LMC	LMC 2	SMC
$E_{FUV-NUV}/E_{B-V}$	0.11	1.08	2.00	4.60
$A_{FUV}/E_{B-V}$	8.06	8.57	9.02	12.68
$A_{NUV}/E_{B-V}$	7.95	7.49	7.02	8.08
$A_U/E_{B-V}$	4.72	3.96	4.11	4.61
$A_B/E_{B-V}$	4.02	3.26	3.46	3.85
$A_V/E_{B-V}$	3.08	2.34	2.54	2.93
$E_{U-B}/E_{B-V}$	0.70	0.70	0.66	0.76

<sup>a</sup>values derived using the standard Milky Way extinction curve from Cardelli et al. (1989): “MW”, using the curve of Misselt et al. (1999) for sightlines in LMC2 (“LMC2”), and using the average LMC extinction curve outside the LMC 2 region (“LMC”) and the UV-steep extinction curves for SMC sightlines (“SMC”) by Gordon & Clayton (1998). The quantities for each broad-band are derived by applying the filter passbands to progressively reddened model atmospheres for stars with  $T_{\text{eff}}$  between 30,000K and 15,000K, and comparing unreddened and reddened model colors with  $E_{B-V}=0.4$ . The mean values are given, the dispersion is always less than 1% within this  $T_{\text{eff}}$  range.

Table 2. List of clusters included in the GUVcat footprint (electronic only, sample shown here)

name	ra	dec	central radius	broad type	cluster status	cluster type
IC4499	225.076996	-82.213997	0.085000	G	O	GLO

Table 3. List of galaxies larger than 1' included in the GUVcat footprint (electronic only, sample shown here)

name	type	ra degrees	dec degrees	v3k km/sec	vlg km/sec	P.A. degrees	inclination degrees	log(D <sub>25</sub> ) (0.1 arcmin)	log(D <sub>25</sub> error) (0.1 arcmin)	log(R <sub>25</sub> ) D <sub>25</sub> /d <sub>25</sub>	log(R <sub>25</sub> error)
UGC12889	G	0.0070005	47.27450	4751	5319	163.5	53.4	1.27	0.03	0.20	0.03

Table 4. List of AIS GALEX fields (*Coadds* and *Visits*) used to construct the GUVcat\_AIS catalog

Field ( <i>photoextractID</i> )	RA center degrees ( <i>avaspra</i> )	Dec center degrees ( <i>avaspdec</i> )	<i>l</i> center degrees	<i>b</i> center degrees	FUV exp.time (seconds) ( <i>ferptime</i> )	NUV exp.time (seconds) ( <i>neaptime</i> )	C or V
6370915756560875520	291.449459	75.146935	106.972770	23.963759	219.050	219.050	<i>coadd</i>
6370915757634617344	273.010299	80.131423	111.833168	28.552309	213.000	213.000	<i>coadd</i>
6370915758708359108	282.810539	78.033136	109.575259	26.360347	251.000	251.000	<i>coadd</i>
6370915759782100992	278.835416	78.547001	110.147665	27.387182	216.000	216.000	<i>coadd</i>
6370915760855842816	273.760205	79.023568	110.744419	28.396397	198.000	198.000	<i>coadd</i>
...	...	...	...	...	...	...	...
6370915708343156736	257.1537508	71.986534	103.457631	33.558659	109.000	109.000	<i>visit</i>
...	...	...	...	...	...	...	...

Note. — Table 4 is published in its entirety in the electronic edition. A portion is shown here for guidance regarding its form and content. In total, 28067 *coadds* and 1468 *visits* are used to build GUVcat\_AIS.

Table 5. List of AIS eliminated *bad coadds*, and their associated visits

<i>Coadd</i> ID (photoextractID)	<i>Coadd</i> RA (degrees)	<i>Coadd</i> Dec (degrees)	<i>Coadd</i> lon (degrees)	<i>Coadd</i> lat (degrees)	<i>Coadd</i> exp.time (sec)		<i>Visit</i> ID (photoextractID)	<i>Visit</i> RA (degrees)	<i>Visit</i> DEC (degrees)	<i>Visit</i> exp.time	
					FUV	NUV				FUV (sec.)	NUV (sec.)
6370915845681446912	257.195457	71.984578	103.457631	33.558659	109.000	267.000	6370915708276047872	257.490785	71.946748	0.000	62.000
6370915845681446912	257.195457	71.984578	103.457631	33.558659	109.000	267.000	6370915708309602304	257.051516	72.006587	0.000	96.000
6370915845681446912	257.195457	71.984578	103.457631	33.558659	109.000	267.000	6370915708343156736	257.153751	71.986534	109.000	109.000
6370950948449157120	250.541348	70.399218	102.543859	36.089296	171.000	350.050	6370950811043758080	250.893395	70.436709	0.000	75.050
6370950948449157120	250.541348	70.399218	102.543859	36.089296	171.000	350.050	6370950811077312512	250.614435	70.469918	0.000	104.000
6370950948449157120	250.541348	70.399218	102.543859	36.089296	171.000	350.050	6370950811110866944	250.340422	70.356973	91.000	91.000
6370950948449157120	250.541348	70.399218	102.543859	36.089296	171.000	350.050	6370950811144421376	250.346796	70.319619	80.000	80.000
...	...	...	...	...	...	...	...	...	...	...	...

Note. — Table 5 is published as online data only. Note: the 640 *badcoadds* were included in BCScat, prior to our discovery of the database improper coadding of non-overlapping *visits*; they are not used in GUVcat, and their corresponding *visits* with both FUV and NUV exposure times > 0 are used instead (1468 out of 2004 total).



Table 6—Continued

latitude range	#sources total	#sources with grank =0	#sources with grank =-1	% sources with grank =0	% sources with grank =-1	area (deg <sup>2</sup> )	band	none	1	2	4	8	16	32	64	128	256	512	
40.35S	3628761	3456338	171585	838	95.25	4.73	0.023	1115.4	1190891	51189	86347	22718	444204	1173	0	35154	92925	124	
							NUV:	2512707											
							FUV:	3328898	0	0	3615	224	0	0	1383	0	262	294907	0
45.40S	3438189	3287766	149958	465	95.62	4.36	0.014	1058.0	1034355	42202	78427	17853	372865	2093	0	28284	95120	51	
							NUV:	2435514											
							FUV:	3144125	0	0	3379	387	0	0	2256	0	265	288448	0
50.45S	3210828	3054911	154880	1037	95.14	4.82	0.032	957.5	929025	37294	65412	17132	338423	2530	0	27296	83680	89	
							NUV:	2366844											
							FUV:	2932586	0	0	2629	267	0	0	1054	0	160	274610	0
55.50S	2936108	2786459	147733	1916	94.90	5.03	0.065	885.6	826472	30788	58111	14007	303229	1437	0	162	235095	18	
							NUV:	2252162											
							FUV:	2696422	0	0	2172	205	0	0	2546	0	162	235095	0
60.55S	2825703	2694479	130287	937	95.36	4.61	0.033	829.0	709768	27170	48545	14823	260102	3318	0	22550	71974	32	
							NUV:	2108224											
							FUV:	2578445	0	0	1991	167	0	0	656	0	113	244689	0
65.60S	2358898	2260825	97496	577	95.84	4.13	0.024	672.8	616894	24339	43856	12815	217084	843	0	19843	64026	19	
							NUV:	2098459											
							FUV:	2146308	0	0	1754	169	0	0	101	0	46	210770	0
70.65S	2181934	2082443	99008	483	95.44	4.54	0.022	620.9	489657	18926	35212	8410	167698	153	0	13456	56966	31	
							NUV:	1777379											
							FUV:	1987819	0	0	1263	127	0	0	160	0	76	192733	0
75.70S	1695985	1624317	71484	184	95.77	4.21	0.011	471.7	439389	17260	31733	8414	151401	192	0	13195	55032	15	
							NUV:	1655414											
							FUV:	1539154	0	0	979	79	0	0	136	0	59	155726	0
80.75S	1169851	1111405	57573	873	95.00	4.92	0.075	333.0	336714	12705	24818	5251	115650	249	0	8421	44232	3	
							NUV:	1292244											
							FUV:	1060612	0	0	651	41	0	0	223	0	48	108422	0
85.80S	811212	767146	43119	947	94.57	5.32	0.117	211.5	221460	8616	16997	3331	78678	225	0	5719	29585	4	
							NUV:	903018											
							FUV:	728465	0	0	540	31	0	0	198	0	7	82066	0
90.85S	227334	217689	9574	71	95.76	4.21	0.031	66.4	151325	5570	13579	3201	51800	454	0	4989	43363	18	
							NUV:	623816											
							FUV:	207506	0	0	111	3	0	0	0	0	3	6720	0
Total	82992086	79549861	3431053	11172	95.85	4.13	0.01	24790.3	39773	1681	3415	509	13344	25	0	902	5436	0	
							NUV:	178466											
							FUV:	76359225	0	0	111	3	0	0	0	0	3	19720	0
							NUV:	56214879											

Note. — GALEX artifact flags :

- Artifact 1 (1):(edge) Detector bevel reflection (NUV only).
- Artifact 2 (2):(window) Detector window reflection (NUV only).
- Artifact 3 (4):(dichroic) Dichroic reflection.
- Artifact 4 (8):(varpix) Variable pixel based on time slices.
- Artifact 5 (16):(brtedge) Bright star near field edge (NUV only).
- Artifact 6 (32):(detector rim (annulus) proximity (>0.6 deg from field center).
- Artifact 7 (64):(dimask) dichroic reflection artifact mask flag.
- Artifact 8(128):(varmask) Masked pixel determined by varpix.
- Artifact 9(256):(hotmask) Detector hot spots.
- Artifact 10(512):(yaghost) Possible ghost image from YA slope.

Table 7. Catalog Source Statistics. UV colors

latitude	#sources	density (# /deg <sup>2</sup> )	# FUV	fraction (#FUV/#NUV)	#sources FUV-NUV ≤ 0	#sources FUV-NUV ≤ 0.5	#sources in galaxies	#sources in clusters	#sources not MC	#sources ≤ 15° from LMC	≤ 10° from SMC
85_90N	249745	3716.58	36434	0.15	10751	24240	316	8643	249745	0	0
80_85N	575444	2814.77	86642	0.15	23838	56095	375	21553	575444	0	0
75_80N	1044253	3061.59	130726	0.13	38373	85756	1386	2607	1044253	0	0
70_75N	1465351	3024.87	195794	0.13	56013	127660	2175	305	1465351	0	0
65_70N	1703241	2988.98	238919	0.14	66078	154227	1351	280	1703241	0	0
60_65N	2098214	3191.04	292232	0.14	81716	188597	1347	0	2098214	0	0
55_60N	2593208	3271.72	337085	0.13	96573	218088	2233	0	2593208	0	0
50_55N	2684044	2986.87	314592	0.12	91570	203731	1425	0	2684044	0	0
45_50N	3235658	3238.55	359081	0.11	106576	232645	1409	976	3235658	0	0
40_45N	3621419	3247.02	362529	0.10	109455	233388	2258	708	3621419	0	0
35_40N	3724140	3175.61	341953	0.09	100999	215049	1601	1363	3724140	0	0
30_35N	3887581	3158.53	321160	0.08	93943	196661	2799	19836	3887581	0	0
25_30N	3923424	3334.07	290238	0.07	84044	171420	1621	1876	3923424	0	0
20_25N	3830858	3464.68	251682	0.07	69040	139172	1398	4614	3830858	0	0
15_20N	2813302	2882.87	126863	0.05	29719	49576	854	7159	2813302	0	0
10_15N	3417929	4346.37	185024	0.05	48188	90471	2078	15187	3417929	0	0
05_10N	1129788	3109.13	53793	0.05	9270	15451	147	3323	1129788	0	0
00_05N	137477	2429.08	11771	0.09	1199	3619	0	1473	137477	0	0
05_00S	98225	2246.47	6756	0.07	681	1762	0	629	98225	0	0
10_05S	576514	2838.62	25939	0.04	5375	8977	33	2630	576514	0	0
15_10S	1885871	3865.60	73420	0.04	20202	30698	48693	2576	1885871	0	0
20_15S	2980587	3967.39	127231	0.04	38069	63299	74678	24730	2954498	26089	0
25_20S	3296612	3602.23	170977	0.05	53134	95767	5211	9308	3130822	165790	0
30_25S	3662226	3509.82	248345	0.07	73965	148739	86561	5099	3326385	335841	0
35_30S	3872172	3436.90	342725	0.09	95991	210826	217832	7626	3391602	472916	7688
40_35S	3628761	3253.33	333036	0.09	99801	213257	78466	1054	3150549	337319	181294
45_40S	3438189	3249.72	379787	0.11	111606	248892	47417	4920	2842873	303802	355523
50_45S	3210828	3353.38	376489	0.12	109139	244447	27606	3436	2831925	67392	312887
55_50S	2936108	3315.46	369087	0.13	105669	238995	1637	12324	2797762	0	138346
60_55S	2825703	3408.57	433883	0.15	117038	277066	1713	33317	2825703	0	0
65_60S	2358898	3506.30	385773	0.16	101852	245762	1833	82	2358898	0	0
70_65S	2181934	3514.37	354422	0.16	94703	226806	1163	993	2181934	0	0
75_70S	1695985	3595.28	291753	0.17	76879	186544	658	0	1695985	0	0
80_75S	1169851	3512.67	208792	0.18	54909	133938	694	1728	1169851	0	0

Table 7—Continued

latitude	#sources	density (# /deg <sup>2</sup> )	# FUV	fraction (#FUV/#NUV)	#sources FUV-NUV ≤ 0	#sources FUV-NUV ≤ 0.5	#sources in galaxies	#sources in clusters	#sources not MC	#sources ≤ 15° from LMC	≤ 10° from SMC
85_80S	811212	3835.03	141506	0.17	36981	90073	321	1240	811212	0	0
90_85S	227334	3423.16	38041	0.17	10449	24905	162	582	227334	0	0
Total:	82992088	1673.85	8244480	0.10	2323788	5096599	619451	202177	80393016	1709149	995738

## A. Appendix A. Criteria for Identifying and Removing Duplicate Measurements

The GALEX database in the MAST archive contains all existing measurements. For sources with repeated AIS observations (e.g. where different fields overlap, or the same field was repeated), we removed duplicate measurements as follows, to produce a unique source catalog. GALEX sources *within 2.5" of each other but from different observations* were considered duplicates. In such cases, the measurement from the observation with the longest exposure time (sum of FUV and NUV exposures) was retained, and - in cases of equal exposure time - the one closest to the center of the field in its parent image.

The choice of a 2.5" match radius was based on several considerations. According to the archive documentation, the accuracy of GALEX source positions is of 0.32/0.34" (NUV/FUV) in the GR7 data<sup>7</sup> and slightly worse, especially in FUV, in previous data. The GALEX pipeline uses a complicated probability algorithm to match FUV sources to the NUV sources of the same observation. In short, NUV and FUV matches are allowed up to 7" . We have examined statistically the tags informative of the FUVxNUV match process. Fig. 4 shows the distribution of the separation between FUV and NUV position for a 2million source subsample of the database, as a whole and divided by cuts in match *probability* (as defined by the pipeline algorithm). Our choice of a 2.5" match radius to define duplicates corresponds statistically to a FUVxNUV match *probability* >0.3, and is consistent with the early versions of our catalogs (Bianchi et al. (2011a, 2014a)), where it was found from other tests to be a good compromise between not excluding real sources and not retaining duplicate measurements. GALEX astrometry is more accurate than 2.5" , but the deblending of sources closer than this separation is not always robust due to the instrument resolution ( $\approx 4.2/5.3''$  , FUV/NUV). This was discussed in Section 4.2. In general, we expect most science applications of this catalog to be restricted to point sources, for which the chosen limit is appropriate.

While the criterion is simple in principle, we add here some important clarifications which were not described in the previous versions of the catalog, and are relevant for any work requiring merging of overlapping observations. To identify duplicates, and eventually remove them, we search the master catalog around the position of each source, within the chosen match radius. If there is no other entry within the match radius of 2.5" , we assign to the source "*grank=0*". Thus, all sources with *grank* = 0 are unique (i.e., have only one

---

<sup>7</sup>the current GALEX database is called "GR6plus7" because not all data have been reprocessed yet, the latest version of the pipeline was used only for the GR7 addition

measurement) also in the original AIS database.<sup>8</sup> If within the match radius around a source “i” we find other sources, measured in a different observation, we assign  $grank=1$  to the best measurement of this group, the “primary” (which will be retained in the final catalog when duplicates are removed); the best measurement is the one with longest exposure, or - for equal exposure - closer to the field center in its parent observation; we assign  $grank=2,3,\dots$  to other sources within  $2.5''$  of the primary, ranked in order of distance from the primary. To keep track of duplicate measurements, since only the primary is retained in the end, we added a tag  $ngrank$ , indicating the number of matches to the primary (including the primary itself), and  $primgid$ , the identifier of the primary (the source with  $grank=1$ ) to which the sources with  $grank>1$  are associated. This basic definition is simple. However, there may happen to be sources - let’s say, a source “j” - farther than  $2.5''$  from the primary “i”, therefore not included in its group, but closer than  $2.5''$  to a source with  $grank>1$  in the group of the primary “i”. If the source previously assigned  $grank>1$  (with respect to source “i”), has better exposure time than its neighbor “j”, its  $grank$  cannot be reclassified to  $=1$  because it does not satisfy the primary criterion with respect to the (better) primary “i”. Therefore, the new source “j” must be retained in the catalog because it’s farther than  $2.5''$  from “i”, but we set its  $grank = -1$  (instead of  $=1$ ), to indicate that another source within  $2.5''$  would have been a primary with respect to “j”, according to our “best measurement” criteria, if it were not a secondary with respect to another, better primary. The  $grank>1$  neighbor in our example is given  $ngrank=-89$ , so it can be identified in the master catalog as a potential primary (with respect to source “j”) which could not be retained in the unique-source catalog because it was a secondary with respect to source “i”. If, instead, source “j” has longer exposure than its neighbor with previous  $grank>1$  but shorter exposure than source “i”, for the source with  $grank>1$  which is a secondary associated to “i” (its  $primgid$  tag indicates the  $objid$  of its primary “i”), we still want to retain the information that there is another source (“j”) within the match radius from it. This information is given in tag  $groupid$ , where all  $objid$ ’s of sources within the match radius are concatenated. Also, tag  $ngrank$  for source “j” indicates the number of all sources within the match radius (including the  $grank>1$  secondary associated to source “i”) but fewer secondaries than its  $ngrank$  will have  $primgid$  equal to  $objid$  of source “j”. This is easier to understand from some examples, shown in Figure 7. Such variety of cases may seem irrelevant subtleties for users of the final catalog, but is worth mentioning; in fact, any code performing associations of repeated measurements

---

<sup>8</sup>we recall that GUVcat AIS only includes the AIS exposures, for homogeneity of exposure depth across the catalog. Some regions were observed repeatedly with deeper exposures, see Bianchi (2014), therefore some AIS sources may have additional observations in other surveys, with longer exposure times. A unique-source catalog at MIS-depth was published by Bianchi et al. (2014a). Deeper exposures will be addressed in a future work.

must include provisions for such cases, and more odd (and rare) situations, otherwise more sources will be eliminated than it is necessary, or wrong associations will result. A code simply performing rank assignment looking for neighbors of each source sequentially, and not accounting for intersecting groups, would eliminate duplicates inconsistently among the sample.

With these -or any other - criteria to define duplicates, there may be sources which are within the match radius of more than one primary, the primaries being more distant than 2.5'' from each other. The assigned primary to each secondary, according to our standard recipe, is the one with the longest exposure time (best measurement) as explained above. For completeness, we also include in the master catalog the tags *grankdist*, and *primgiddist*, the latter indicates the closest primary to the source, and *grankdist* is its ranking with respect to the closest primary. This may be different from the "best-measurement" primary (*primgid*). With the distance-criterion tags, a secondary may be reassigned from the original primary (best measurement, *primgid*) to the closest primary (*primgiddist*) and therefore the number of secondaries for each primary may differ from *ngrank*; we record this number in the tag *nkgrank*. These details only concern users who wish to delve in the master catalog GUVcat\_AISplus, where we include all AIS measurements from the archive, and create these tags so that one can chose the primary sources only (*grank*=0, 1 or -1), i.e. removing all duplicates at once, and obtain a catalog where each source is counted only once, or viceversa examine repeated measurements of AIS sources. GUVcat\_AISplus is also available from MAST's casjobs.

However, for most purposes only the primary sources are needed, and it is not convenient for a user to download all measurements and having to apply cuts later using our *grank* tags described above. GUVcat\_AIS contains only 'unique sources', with duplicate measurements removed. This is extracted from the master catalog GUVcat\_AISplus by retaining only sources with *grank*=0, 1 or -1.

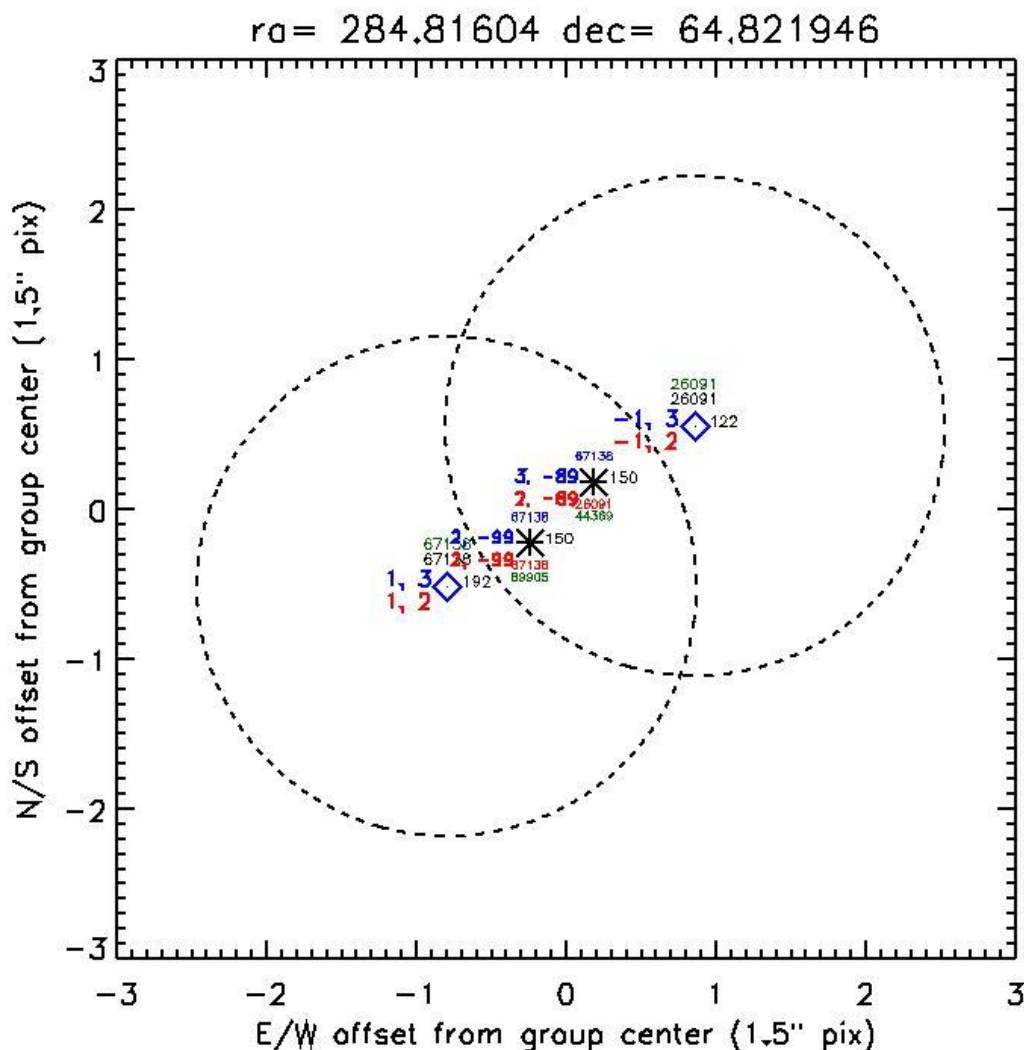


Fig. 7.— Examples of multiple observations for the same source. The source at the center of the lower-left circle (blue diamond, id=67138) has the best measurement out of three within  $2.5''$  from its position (dashed circle); therefore it is assigned  $grank=1$ ,  $ngrank=3$  (blue numbers at the left). Its closest neighbor has  $grank=2$ ,  $ngrank=-99$  (because it is not a primary). The second closest, with id = 44309, has  $grank=3$ , but  $ngrank=-89$  because it also falls within  $2.5''$  of another source (id=26091) which is further than  $2.5''$  from the first primary and has exposure time shorter than source 44309. Object id=26091 is therefore assigned  $grank=-1$ , because it cannot be discarded as duplicate of the first primary, but has a nearby source which has a better measurement but cannot be “primary” because it is secondary with respect to a better primary. The black numbers to the right of the sources are exposure time in seconds. The  $grank$  tag is used to eliminate secondaries in the unique-source catalog. The red numbers show the values of the same tags if we used instead a distance criterion and associate secondaries to the closest primary rather than to the “best” primary. In that case, each of these two primaries would get one secondary. Note that  $grank$  for primaries would not change.



## B. Appendix B. Description of The Catalogs' Columns

Below we list the tags included in the online catalogs presented in this paper, and available at <http://dolomiti.pha.jhu.edu/uvsky/#GUVcat> , as well as from MAST casjobs and SIMBAD/Vizier. The columns of greatest interest in most cases are in bold in the Table below. The first sets of tags are propagated from the pipeline database, and give information on the source photometry; tags *CORV* and beyond, indicated in italics, are generated by us and described in this paper; some indicate whether the source has duplicate (AIS) measurements, that have been removed (Section A, or flagged if one uses the 'plus' catalog). The last two tags indicate whether the source is in the footprint of a large ( $>1'$ ) object (Section 6.1).

Table 8. Catalog Columns

Tag	Description
photoextractid	Pointer to photoExtract Table (identifier of original observation on which the measurement was taken)
mpstype	which survey (e.g. "MIS", or "AIS", ...)
avaspra	R.A. of center of field where object was measured
avaspdec	Decl. of center of field where object was measured
<b>objid</b>	GALEX identifier for the source
<b>ra</b>	source's Right Ascension (degrees).
<b>dec</b>	source's Declination (degrees)
<b>glon</b>	source's Galactic longitude (degrees)
<b>glat</b>	source's Galactic latitude (degrees)
tilenum	"tile" number
img	image number (exposure # for <i>visits</i> )
subvisit	number of subvisit if exposure was divided
fov_radius	distance of source from center of the field in which it was measured
type	Obs.type (0=single,1=multi)
band	Band number (1=nuv,2=fuv,3=both)
<b>e_bv</b>	E(B-V) Galactic Reddening (from Schlegel et al. 1998 maps)
istherespectrum	Does this object have a (GALEX) spectrum? Yes (1), No (0)
chkobj_type	Astrometry check type
<b>fuv_mag</b>	FUV calibrated magnitude
<b>fuv_magerr</b>	FUV calibrated magnitude error
<b>nuv_mag</b>	NUV calibrated magnitude
<b>nuv_magerr</b>	NUV calibrated magnitude error
fuv_mag_auto	FUV Kron-like elliptical aperture magnitude
fuv_magerr_auto	FUV RMS error for AUTO magnitude
nuv_mag_auto	NUV Kron-like elliptical aperture magnitude
nuv_magerr_auto	NUV RMS error for AUTO magnitude
fuv_mag_aper_4	FUV Magnitude aperture ( 8 pxl )
fuv_magerr_aper_4	FUV Magnitude aperture error ( 8 pxl )
nuv_mag_aper_4	NUV Magnitude aperture ( 8 pxl )
nuv_magerr_aper_4	NUV Magnitude aperture ( 8 pxl ) error
fuv_mag_aper_6	FUV Magnitude aperture ( 17 pxl )
fuv_magerr_aper_6	FUV Magnitude aperture ( 17 pxl ) error
nuv_mag_aper_6	NUV Magnitude aperture ( 17 pxl )
nuv_magerr_aper_6	NUV Magnitude aperture ( 17 pxl ) error
<b>fuv_artifact</b>	FUV artifact flag (logical OR near source)
<b>nuv_artifact</b>	NUV artifact flag (logical OR near source)
fuv_flags	Extraction flags
nuv_flags	Extraction flags
fuv_flux	FUV calibrated flux (micro Jansky)
fuv_fluxerr	FUV calibrated flux (micro Jansky) error
nuv_flux	NUV calibrated flux (micro Jansky)
nuv_fluxerr	NUV calibrated flux (micro Jansky) error
fuv_x_image	Object position along x
fuv_y_image	Object position along y
nuv_x_image	Object position along x

Table 8—Continued

Tag	Description
nuv_y_image	Object position along y
fuv_fwhm_image	FUV FWHM assuming a gaussian core
nuv_fwhm_image	NUV FWHM assuming a gaussian core
fuv_fwhm_world	FUV FWHM assuming a gaussian core (WORLD units)
nuv_fwhm_world	NUV FWHM assuming a gaussian core (WORLD units)
nuv_class_star	S/G classifier output
fuv_class_star	S/G classifier output
<b>nuv_ellipticity</b>	1 - B.IMAGE/A.IMAGE
<b>fuv_ellipticity</b>	1 - B.IMAGE/A.IMAGE
nuv_theta_J2000	Position angle (east of north) (J2000)
nuv_errtheta_J2000	Position angle error (east of north) (J2000)
fuv_theta_J2000	Position angle (east of north) (J2000)
fuv_errtheta_J2000	Position angle error (east of north) (J2000)
fuv_ncat_fwhm_image	FUV FWHM.IMAGE value from -fd-ncat.fits (px)
fuv_ncat_flux_radius_3	FUV FLUX_RADIUS #3 (-fd-ncat)(px)[0.80]
nuv_kron_radius	Kron apertures in units of A or B
nuv_a_world	Profile RMS along major axis (world units)
fuv_kron_radius	Kron apertures in units of A or B
fuv_b_world	Profile RMS along major axis (world units)
nuv_weight	NUV effective exposure (flat-field response value) in seconds at the source position (center pixel) given alpha_j2000, del
fuv_weight	FUV effective exposure
prob	probability of the FUV x NUV match
sep	separation between FUV and NUV position of the source in the same observation
nuv_poserr	[arcseconds] position error of the source in the NUV image
fuv_poserr	[arcseconds] position error of the source in the FUV image
IB_POSERR	[arcseconds] inter-band position error in arcseconds
NUV_PPERR	[arcseconds] NUV Poisson position error (the part of the position error due to counting statistics)
FUV_PPERR	[arcseconds] FUV Poisson position error (the part of the position error due to counting statistics)
<i>CORV</i>	whether the source comes from a <i>Coadd</i> or <i>Visit</i>
<i>GRANK</i>	grank=0 if the are no other sources (from different observations) within 2.5'' grank=1 if this is the best (see text) source of >1 sources within 2.5'' grank=-1 if this is a primary but has a better source within 2.5'' grank =n (n>1) is this is the n <sup>th</sup> source within 2.5'' of the primary
<i>NGRANK</i>	if this is a primary, number of sources within 2.5'' (otherwise, 99 or 89, see text)
<i>PRIMGID</i>	objid of the primary (only of use for the 'plus' catalog)
<i>GROUPEGID</i>	objid's of all sources (AIS) within 2.5'' , concatenated by "+"
<i>GRANKDIST</i>	as for grank, but based on distance criterion
<i>NGRANKDIST</i>	as for ngrank, but based on distance criterion
<i>PRIMGIDDIST</i>	as for primgid, but based on distance criterion (objid of the closest primary rather than the best primary)(only of use for the 'plus' catalog)
<i>GROUPEGIDDIST</i>	as GROUPEGID, but based on distance criterion
<i>GROUPEGIDTOT</i>	objid's of all sources within 2.5''
<i>DIFFFUV</i>	mag difference between primary and secondary (only of use for the 'plus' catalog)
<i>DIFFNUV</i>	mag difference between primary and secondary (only of use for the 'plus' catalog)
<i>DIFFFUVDIST</i>	mag difference between closest primary and secondary (only of use for the 'plus' catalog)
<i>DIFFNUVDIST</i>	mag difference between closest and secondary (only of use for the 'plus' catalog)

### C. Appendix C. Odd Fields and Artifacts

In Section 6.2 we mentioned the different artifacts flagged by the GALEX source extraction pipeline, and Table 6 gives the statistics of sources with artifact flags. Fig. 8 shows examples of ghost reflections from bright sources, in FUV and NUV, and of other types of artifacts. We use as example one of the fields where there is also an apparent mismatch in coordinates between FUV and NUV detections (Section 5.2).

The definition of artifacts can be found in the documentation<sup>9</sup> and is reported in the footnote of Table 6.

---

<sup>9</sup>[http://www.galex.caltech.edu/wiki/Public:Documentation/Chapter\\_8#Artifact.Flags](http://www.galex.caltech.edu/wiki/Public:Documentation/Chapter_8#Artifact.Flags)

Table 8—Continued

Tag	Description
<i>SEPAS</i>	separation (arcsec) between primary and secondary
<i>SEPASDIST</i>	separation (arcsec) between primary (distance criterion) and secondary
<b>INLARGEOBJ</b>	is the source in the footprint of an extended object? if not, INLARGEOBJ=N if yes, INLARGEOBJ= XX:name-of-the-extended-object ; where XX=GA (galaxy), GC (globular cluster), OC (open cluster), SC (other stellar clusters)
<b>LARGEOBJSIZE</b>	size of the extended object; LARGEOBJSIZE = 0. if INLARGEOBJ=N, otherwise LARGEOBJSIZE= D25 for galaxies and 2xR <sub>1</sub> for stellar clusters

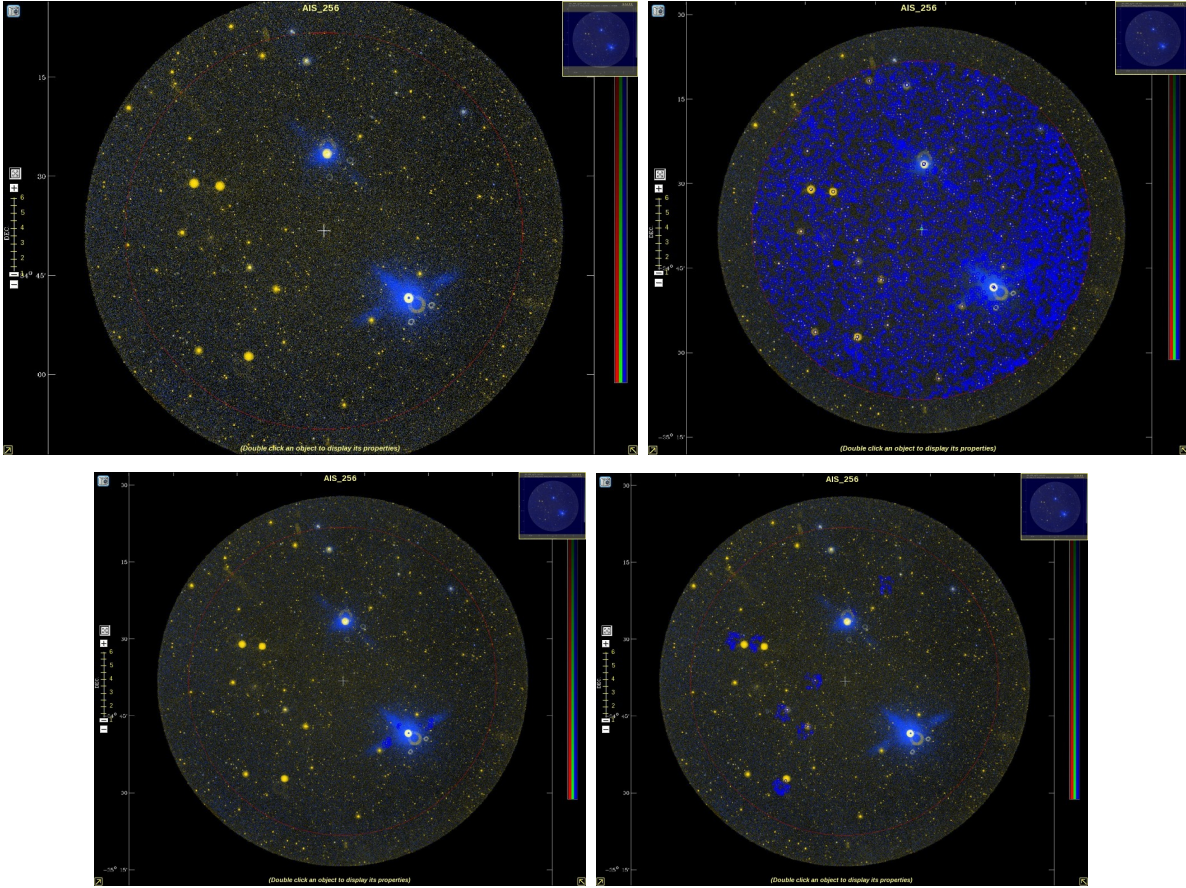


Fig. 8.— GALEX Field AIS.256: the top panels show the entire field with and without pipeline sources overlaid (blue circles, all detections in the central  $1^\circ$ ), combining the FUV (blue) and NUV (yellow) images. The red circle indicates a diameter of  $1^\circ$ . Ghosts from very bright sources are clearly visible as yellow rings offset from the source position for NUV, and as extended streaks in FUV. The bottom panels show only the sources with FUV\_artifact=128 (left, ghosts from the bright sources), and with NUV\_artifact=2 (right, ghost rings around bright sources; note that the sources are always plotted as blue circles).

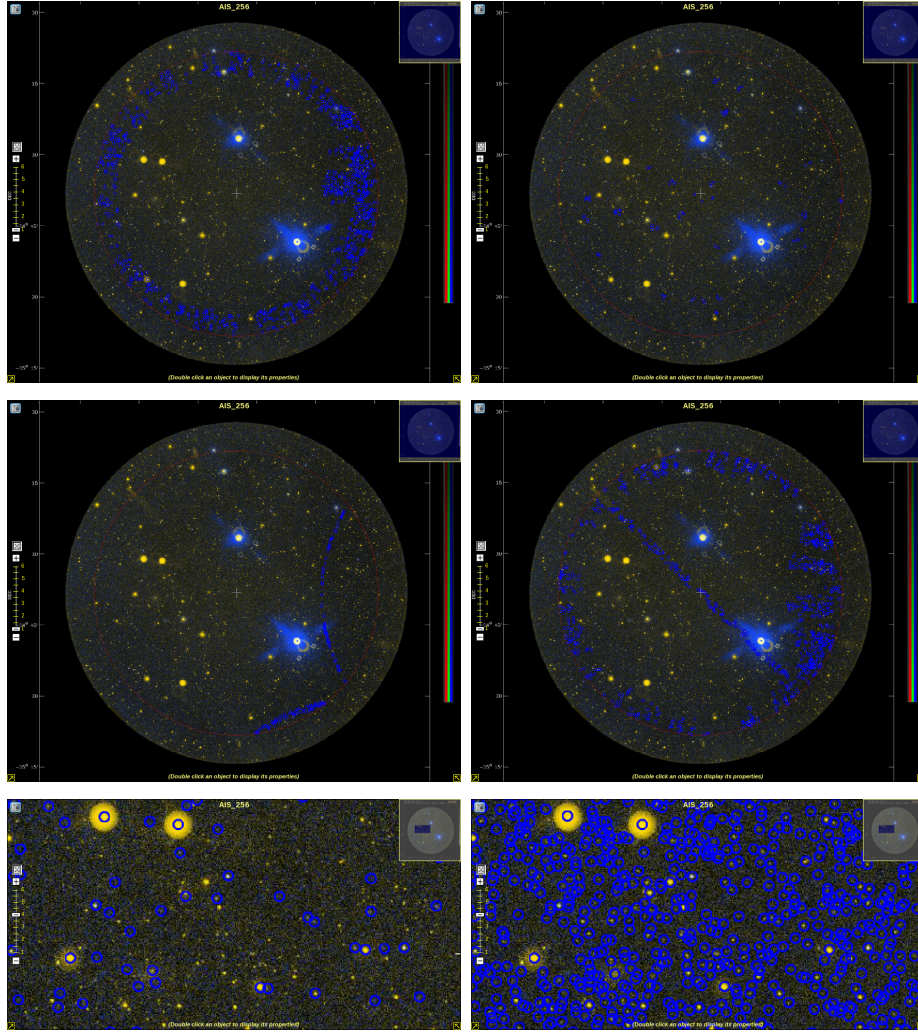


Fig. 8 (Cont.).— Continued from previous. Top: sources affected by  $\text{NUV\_artifact}=1$  (left) and 256 (right: hot spots, taken care of by the pipeline); in the next row, left, sources with rim artifact ( $\text{FUV\_artifact}=32$ ), these are not measured in this image, they come in the database from overlapping visits: they are not included in GUVcat; right: sources with  $\text{NUV\_artifact}=1$  or 16. In the bottom row, we show separately sources detected in FUV (left) and NUV (right). As discussed in the text, this is one of five problematic fields, which represents an extreme example.